

The Meteorologic Magazine

November

range for
The Inter-
scale Initi-
the autumn



Vol. 119 No. 11 Nov. 1970

© Crown copyright 1990.

First published 1990



HMSO publications are available from:

HMSO Publications Centre
(Mail and telephone only)
PO Box 276, London, SW8 5DT
Telephone orders 071-873 9090
General enquiries 071-873 0011
(queuing system in operation for both numbers)

HMSO Bookshops
49 High Holborn, London, WC1V 6HB 071-873 0011 (counter service only)
258 Broad Street, Birmingham, B1 2HE 021-643 3740
Southey House, 33 Wine Street, Bristol, BS1 2BQ (0272) 264306
9-21 Princess Street, Manchester, M60 8AS 061-834 7201
80 Chichester Street, Belfast, BT1 4JY (0232) 238451
71 Lothian Road, Edinburgh, EH3 9AZ 031-228 4181

HMSO's Accredited Agents
(see Yellow Pages)

and through good booksellers

The Meteorological Magazine

November 1990
Vol. 119 No. 1420

551.509.333

Practical extended-range forecasting using dynamical models

S.F. Milton

Meteorological Office, Bracknell

EASTERN MICHIGAN UNIVERSITY
LIBRARY

13 DEC 1990

Summary

SCIENCE & TECHNOLOGY

Real-time ensembles of dynamical model forecasts are now a regular component of the long-range forecasts of temperature and rainfall for the United Kingdom issued on a twice-monthly basis by the Meteorological Office. Results are presented showing the impact of the ensemble technique on predictability, and comparisons are drawn between the skill of this dynamical technique and the current statistical technique. Also discussed is the ability of the ensemble to provide an a priori estimate of forecast skill.

1. Introduction

Since December 1963, twice-monthly forecasts of temperature and rainfall for the month ahead have been produced for the United Kingdom by the Meteorological Office. Until recently, the long-range forecast (LRF) has relied heavily upon statistical techniques to forecast for the period beyond 10 days, commonly referred to as the extended range. The latest of these is the multi-variate analysis (MVA) forecasting technique introduced in 1982 and described in detail by Maryon and Storey (1985), Folland and Woodcock (1986) and Gilchrist (1986). However, the improvements in medium-range skill of numerical weather prediction (NWP) models in the late 1970s and 1980s have led to renewed interest in the dynamical model as a tool for extended-range forecasting, with research into the problem being carried out at most of the major weather-forecasting and climate centres throughout the world.

Since December 1988, real-time, dynamical model forecasts have been made using the ensemble forecast technique, and these have been considered as part of the input to the twice-monthly conferences at which the LRF is decided. The introduction of dynamical model techniques coincided with the forecasts of rainfall and temperature being issued to selected companies in a commercial trial which began in June 1989. This article discusses the practical impact of the dynamical forecasts,

and reviews the current status of dynamical extended-range forecasting at the Meteorological Office.

2. The role of dynamical models

2.1 The ensemble technique

Much of the research into applying dynamical models to the problem of extended-range forecasting has concentrated on the ensemble forecast method proposed by Leith (1974). Detailed accounts of the technique are given by Murphy (1988), but it is worthwhile giving a summary of the major points. Such an ensemble comprises several dynamical model forecasts run from slightly different initial conditions. The rationale of basing extended-range forecasts on ensembles arises from two facts, namely:

- the initial state of the atmosphere can never be measured perfectly, and
- the dynamical equations of motion are non-linear and unstable to small perturbations.

Under condition (a) an ensemble of equally likely initial states can be realized, where each state is consistent with the errors inherent in current observational networks and NWP analyses. Under condition (b) the differences between the initial states grow as the

model forecasts progress until any two states are as different as random states drawn from model climatology and all predictability is lost. Lorenz (1982) estimated this theoretical limit of deterministic predictability to be around 14 days for prediction of instantaneous weather states from a NWP model. The practical limit determined by verifying forecasts against their corresponding analyses was found to be 8–10 days. However, numerous studies have shown cases which remain predictable beyond this limit.

NWP is, therefore, a probabilistic process. The ensemble forms a probability distribution and, providing it is assumed that the states in a large well-sampled ensemble are distributed normally, the ensemble mean represents the 'best-estimate' forecast, and the variance of the probability distribution, or spread of the ensemble members, an estimate of the uncertainty associated with the ensemble mean. When all ensemble members agree (disagree) there is confidence (no confidence) in the prediction. In theory the ensemble should provide a means of identifying those cases which exhibit predictability beyond the deterministic limit. In practice the technique is made less effective by external sources of error due to imperfect model formulation; these force the model to drift towards its own climate, and away from that of the atmosphere, as the forecasts progress. This is discussed in section 4.

If the atmosphere possesses non-Gaussian properties, as is suggested by recent research showing the bimodality in the amplitude of large-scale planetary waves (Sutera 1986), then it may be possible that ensembles will form clusters of states (Murphy and Palmer 1986). In this event, a more probabilistic approach is appropriate, with the ensemble offering a number of possible alternatives to the ensemble mean, each with its own probability of occurrence (Brankovic *et al.* 1990, Déqué 1988, Murphy 1990).

2.2 Real-time ensemble forecasts

Several methods exist for generating the initial states for ensemble forecasts, most involving the addition of suitably chosen perturbations to some reference state, usually the latest operational analysis from a NWP model. Indeed the optimal choice of such perturbations is itself an active research area.

The lagged average forecast (LAF) approach of Hoffman and Kalnay (1983) was adopted for the Meteorological Office ensemble forecasts as it represented the only practical approach to running regular ensemble forecasts given the computational constraints. Each LAF ensemble consists of nine forecasts run from consecutive 6-hourly analyses up to and including the latest operational analysis available. Therefore at the initialization time of the ensemble (corresponding to the latest analysis time or day 0), the first member is a 48-hour forecast, the second a 42-hour forecast, and so on up to the ninth member which is the latest analysis. This distribution of initial states at day 0 is taken to be

representative of the uncertainty in the analysis. The forecast integrated from the latest analysis time (hereafter referred to as the operational dynamical forecast (ODF)) is run for 30 days and the earliest ensemble member for 32 days, so that each member covers the 30 days comprising the forecast period.

The model used is a reduced horizontal-resolution (2° latitude by 2.8° longitude) version of the 15-level, global operational NWP model (Bell and Dickinson 1987). This is in contrast to the real-time ensemble of Murphy and Palmer (1986) where the 11-level general circulation model was used.

In addition to the real-time ensembles a number of hindcast LAF ensembles have been run, and a continuous time-series of forecast ensembles, each separated by 14 days, exists from September 1987 to August 1989. Ensembles for the winters of 1985/86 and 1986/87 have also been run bringing the total number to 65, or 578 individual forecasts. A number of ensembles have less than 9 members owing to operational problems. This is a much larger and more extensive database than used in previous studies, such as the dynamic extended-range forecasts experiments carried out at the National Meteorological Centre (NMC) (Tracton *et al.* 1989).

2.3 Methodology for the LRF

The methods used to produce long-range forecasts of temperature and rainfall in the Meteorological Office are discussed by Folland and Woodcock (1986). Indeed much of their procedure is still pertinent to the issued forecast today, and is outlined below. The MVA method forecasts on a half-monthly basis using linear discriminant equations, whose input is a set of recent atmospheric and sea surface temperature (SST) predictors, to assign probabilities to six pre-determined half-monthly mean-sea-level pressure (MSLP) patterns ('clusters'). These MSLP forecasts are considered along with the dynamical model forecasts to produce a final MSLP forecast for the 3 periods, days 1–5, days 6–15 and days 16–30. In the first period the operational dynamical forecasts from the Meteorological Office and the European Centre for Medium-range Weather Forecasts (ECMWF) figure heavily in the decision-making process. In the second period the forecaster uses the guidance from the days 6–10 of the ECMWF forecast, the nine-member ensemble forecast, and MVA. At days 16–30 the latter two are used exclusively.

Once the MSLP forecasts are decided upon, the temperature and rainfall are derived from 'objective specification equations'. These are multiple regression equations relating temperature anomalies and rainfall (as a percentage of normal) to the predictor variable MSLP, from which the predictors vorticity and the northerly and easterly wind components are derived. Temperature regressions also include the SST anomalies and 1000–500 mb thickness (for days 1–5 only) as additional predictors. The relationships between the

predictor variables and the temperature and rainfall are derived using data from 1951–80. No direct model output is currently used.

The remaining sections describe the extent to which ensemble forecasts are able to provide an accurate prediction of MSLP, as well as provide additional information on the likely skill of a given forecast based upon the ensemble spread.

3. Skill of the dynamical models

3.1 Practical impact of ensemble averaging

For the purposes of this article the anomaly correlation coefficient (ACC) (Miyakoda *et al.* 1972) is the main measure of skill used. Essentially it measures the agreement between forecast and analysis in terms of the phase of the anomaly patterns. A score of +1 represents a skilful forecast (e.g. forecasting and observing positive anomalies in the same location), and a score of -1 an unskilful forecast (e.g. forecasting

positive anomalies when negative anomalies are observed). The scores quoted in the following sections are measured over an area covering the North Atlantic and Europe (30° N– 60° N, 60° W– 40° E), corresponding to the area considered in the LRF. The anomalies are formed with respect to a 1951–80 climatology.

The skill of the dynamical model is shown on a seasonal basis in Fig. 1. This gives the ACC for MSLP measured over consecutive pentad periods of the forecast (days 1–5, 6–10 ... 26–30), for the unweighted ensemble mean, ODF, and the average skill of the individual ensemble members. Pentads are used in preference to the forecast periods to avoid the complication of using different averaging periods. Considering the ODF, all seasons display a steady decrease in skill with ACC falling from values in excess of 0.8 at days 1–5 to near constant values ranging from +0.2 to -0.2 by around days 11–15. Winter appears most skilful with a slower decay in ACC than the other seasons. Autumn is least skilful with ACC becoming

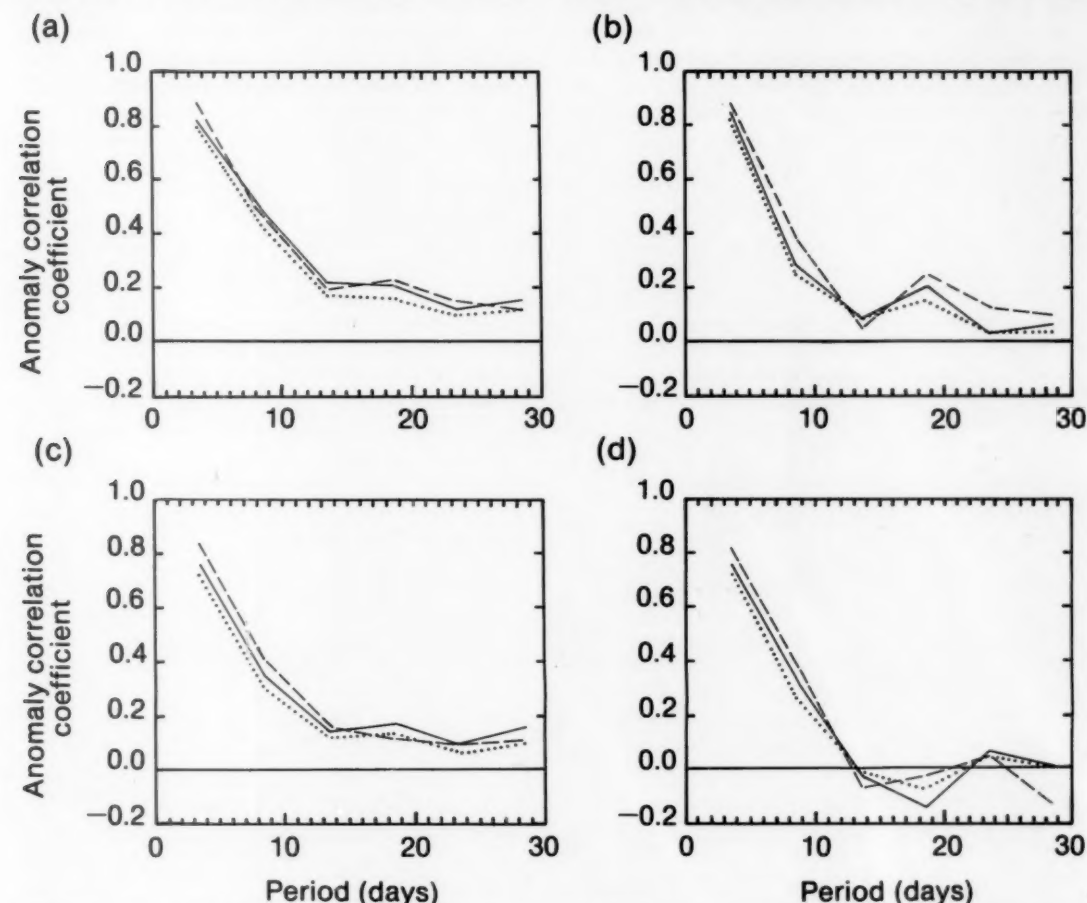


Figure 1. Average MSLP anomaly correlation coefficient for the North Atlantic and Europe for 5-day mean forecast periods plotted at the mid-point of the 5-day means for (a) winter (December–February), (b) spring (March–May), (c) summer (June–August), and (d) autumn (September–November). Continuous lines represent the ensemble mean, dotted lines the average of individual ensemble members and dashed lines the operational dynamical forecast.

negative at days 11–15. These results are typical of the modest levels of skill obtained in extended-range predictions from dynamical models at other centres such as ECMWF and NMC.

In comparison with the ODF the improvement due to ensemble averaging appears rather disappointing with the ensemble mean rarely an improvement over the ODF. As expected from theory (Brankovic *et al.* 1990) the ensemble mean is more skilful than the average skill of the individual members in most periods. However, this improvement is much less than the potential demonstrated by Murphy (1988) using the perfect model approach, where the ensemble is verified against an additional integration of the model taken to represent the real atmosphere. This measures the impact of the ensemble under the assumption that the model possesses no systematic biases.

If we composite the average skill into predictable and unpredictable cases as in Murphy (1990) then the impact of the ensemble averaging is more clearly seen. Fig. 2(a) shows the average ACC for MSLP of the ensemble mean, ODF, and average of the individual members, where ensembles have been assigned to various skill categories according to the average ACC of the individual ensemble members. This clearly shows that when the ensemble possesses above-average skill

(categories B1 and B2) then the ensemble-mean shows a greater improvement over the average ACC of the individual members than is suggested by Fig. 1. In fact in these two top categories the ensemble mean is also, on average, more skilful than the ODF. Fig. 2(b) shows that approximately 55% of the ensembles have ACC above 0.2 at days 6–15, and 15% ACC in excess of 0.6.

3.2 Variability in ensemble skill

Seasonal variations in skill are clearly evident from Fig. 1. However, there is also considerable variation on a case-by-case basis, seasonally, and interannually. It is the case-by-case variations in skill one is attempting to predict using the ensemble spread. To demonstrate this variability the ensemble-mean skill at days 6–15 is plotted as a pseudo time-series as in Fig. 3(a), beginning with the ensemble from 25 November 1985 and ending with that on 14 August 1989. There are considerable fluctuations in skill with ACC ranging from −0.6 to +0.9. The average ACC over all 65 cases is 0.24. The earlier impression of winter as most skilful can clearly be seen, although there are large interannual fluctuations, with the winter of 1988/89 being particularly skilful, compared with the winters of 1985/86 and 1986/87. On average autumn has low skill in this period with three of the worst forecasts appearing in this season. However,

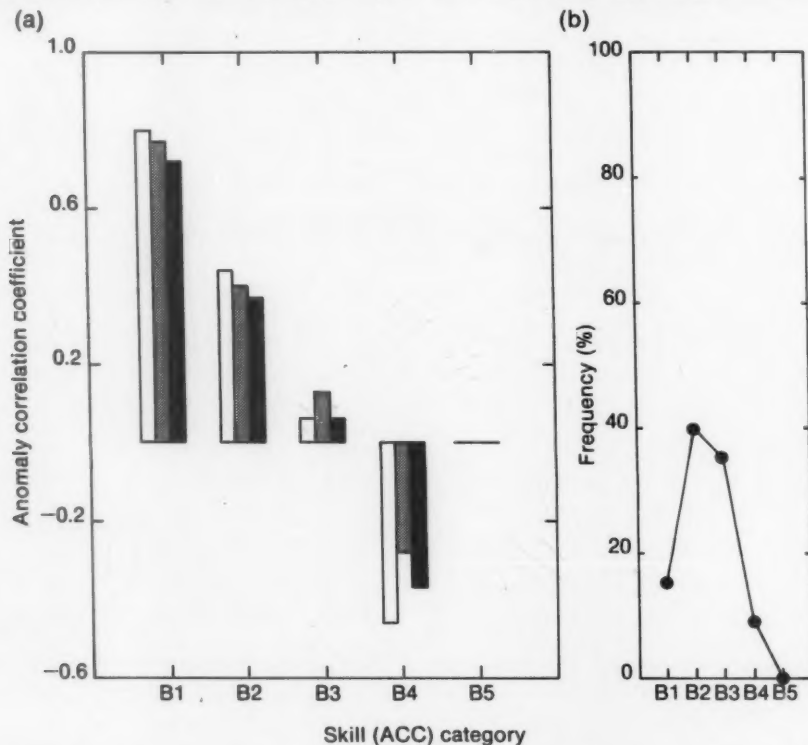


Figure 2. (a) Average MSLP anomaly correlation coefficients (ACC) of the operational dynamical forecast (stippled columns), ensemble mean (unshaded columns), and average of individual ensemble members (solid columns) at days 6–15 over the North Atlantic and Europe, assigned to skill categories (B1–B5) according to the ACC of the individual ensemble members. B1 = $1.0 > \text{ACC} > 0.6$, B2 = $0.6 > \text{ACC} > 0.2$, B3 = $0.2 > \text{ACC} > -0.2$, B4 = $-0.2 > \text{ACC} > -0.6$ and B5 = $-0.6 > \text{ACC} > -1.0$. (b) Frequency of ensembles falling into each skill category.

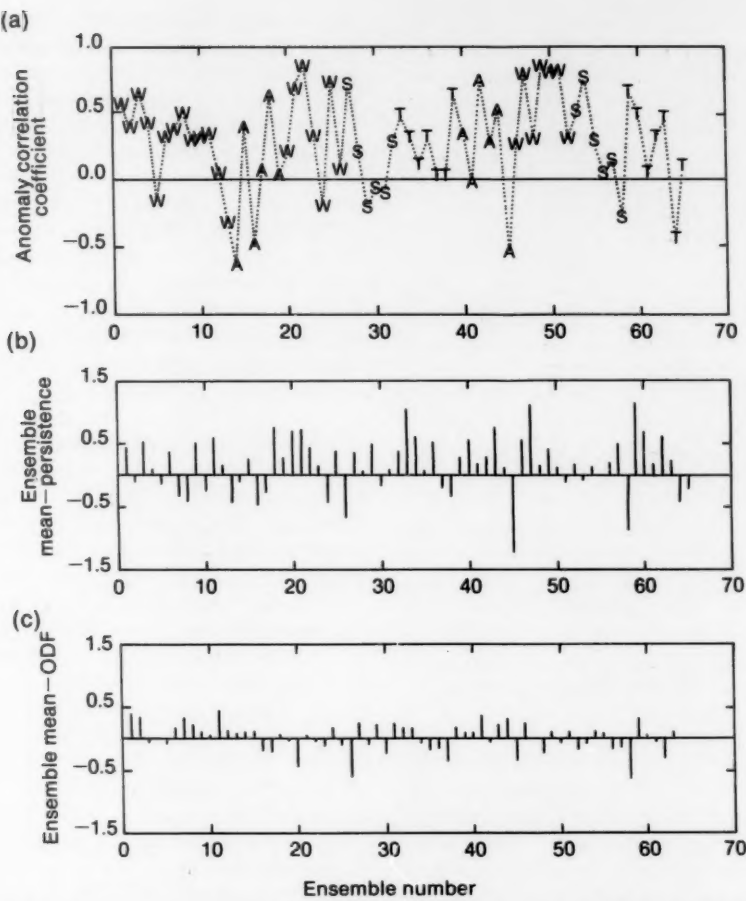


Figure 3. (a) Time series of anomaly correlation coefficients (ACC) for the ensemble mean for MSLP over the North Atlantic and Europe at days 6–15. W = winter, S = spring, T = summer, and A = autumn, for the 65 ensembles 1985–89. (b) As (a) but for the difference in ACC between the ensemble mean and persistence. (c) As (a) but for the difference in ACC between the ensemble mean and the operational dynamical forecast (ODF).

large case-by-case fluctuations are again evident. In contrast, both spring 1988 and 1989 follow similar patterns with the skill dropping rapidly as the season advances, not returning to higher levels until early summer (late May and June).

Figs 3(b) and 3(c) show the differences in ACC between the ensemble mean and persistence/ODF respectively. When this index is positive the ensemble mean is most skilful. Persistence represents a ‘zero-cost’ forecast, and is formed by persisting the anomaly from the 10 days before the analysis time. The ensemble mean is more skilful than persistence on 68% (54%) of occasions at days 6–15 (16–30), and more skilful than the ODF on 57% (43%).

The model performs particularly well during certain persistent episodes in the real atmosphere, such as the winter of 1988/89. However, there are numerous cases where the model skill is very high and persistence is low, such as cases 21, 22, 25 and 47. Fig. 4 shows a 3-point running mean of the ACC for the 52 cases forming a

continuous time-series (cases 14–65). Also plotted is the running mean of persistence. Both of these plots show the large-scale trends in skill, and it can be seen that the ACC of the ensemble forecasts is in some sense modulated by the observed persistence (the overall correlation between the two curves is 0.54, compared with 0.24 for the unsmoothed curves). This is most obvious in winter when persistence and ensemble-mean ACC are maxima, and spring where the decrease in persistence is matched by a decay in ACC of the ensembles; it is most likely a reflection of the model’s inability to undergo low-frequency transitions. Exceptions to the above are summers 1988 (cases 33–39) and 1989 (cases 59–65), where the ensemble-mean ACC, though lower than other seasons, was a significant improvement over persistence.

Finally, it is interesting to consider the degree of variation in skill amongst the individual members of any one ensemble. Fig. 5 presents the ACC for MSLP at days 6–15 for each of the 27 ensembles which make up

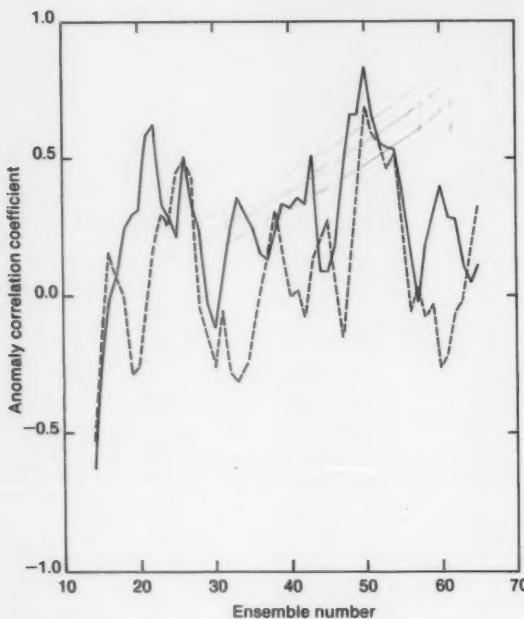


Figure 4. Smoothed anomaly correlation coefficients (ACC) for the 52 ensembles (continuous line) beginning 31 August 1987, and the corresponding persistence ACC scores (dashed line). Smoothing is applied using a 3-point running mean.

the winter set. The histograms show the marked variations in skill for some of the ensembles (e.g. 3 February 1986 and 5 January 1987). In this period it is evident that the ODF is not the most skilful forecast, with 17 out of 27 cases showing the ensemble mean with higher ACC. At days 1–5 the ODF is consistently the best dynamical forecast. This is a consequence of the LAF technique. The perturbations to the initial state represented by the time-lagged ensemble arise from forecast error growth, and such perturbations are generally larger for the earlier ensemble members. Thus, at days 1–5 and 6–10 the members are not *a priori*

equally likely. Hoffman and Kalnay (1983) found that by weighting the individual ensemble members they could make their ensemble mean more skilful than the ODF in these time ranges, and a similar procedure could be applied to the LAF ensembles in an attempt to maximize their usefulness. Beyond the medium range, at days 11–15, the ensemble members are *a priori* equally likely, and no weighting of the members is necessary.

The winter of 1988/89 stands out with high skill and good agreement between ensemble members for four forecasts; a reflection of the persistent, stable, and predictable nature of the pattern which led to a very mild, dry winter (Northcott 1989) leaving many areas of England under drought conditions in the warm summer that followed.

3.3 Dynamical versus statistical forecasts

With the MVA predicting on a half-monthly basis it is difficult to make a direct comparison between the dynamical and statistical inputs to the issued forecasts. However, Table I is an attempt to do this, and compares the scores for MSLP for the two forecasting techniques. The MVA scores are based on the top cluster-pattern (i.e. that with the highest probability) for forecasts covering the half-months from 1986–89. The ACCs for the ensemble mean are based upon a sub-sample of the 65 forecasts covering those ensembles with verification times closest to the MVA half-months. Note that the ensemble forecast for days 6–15 is compared with the MVA forecast for days 1–15, as it is felt that the inclusion of the very skilful days 1–5 from the dynamical forecasts is an unfair comparison. Also the seasons are defined slightly differently from those used in previous sections to agree with the MVA forecasts.

The ensemble-mean predictions averaged over all seasons provide the highest skill out to day 15. This holds for individual seasons except summer where the skill of the ensemble mean is marginally less than MVA, and autumn, where both techniques are poor. For days 16–30 both the ensemble mean and MVA perform

Table I. Anomaly correlations of the top cluster from statistical (MVA) forecasts January 1986 to August 1989 versus the ensemble-mean forecasts available over the same period, measured over a 30-point grid around the United Kingdom (30° W– 20° E, 45° N– 65° N). The first half-month MVA forecasts are compared with days 6–15 of the ensemble forecasts and the second half-month with days 16–30. Each season is composed of four half-months (e.g. winter is Jan1, Jan2, Feb1 and Feb2).

Season	First half-month		Second half-month	
	MVA	Ensemble mean	MVA	Ensemble mean
Winter	0.10	0.34	0.03	0.08
Spring	0.03	0.30	-0.09	-0.13
Pre-summer	0.06	0.25	0.13	0.29
Summer	0.21	0.17	0.04	0.01
Autumn	0.00	-0.02	0.12	-0.29
Pre-winter	0.25	0.43	-0.02	0.27
All seasons	0.11	0.24	0.04	0.04

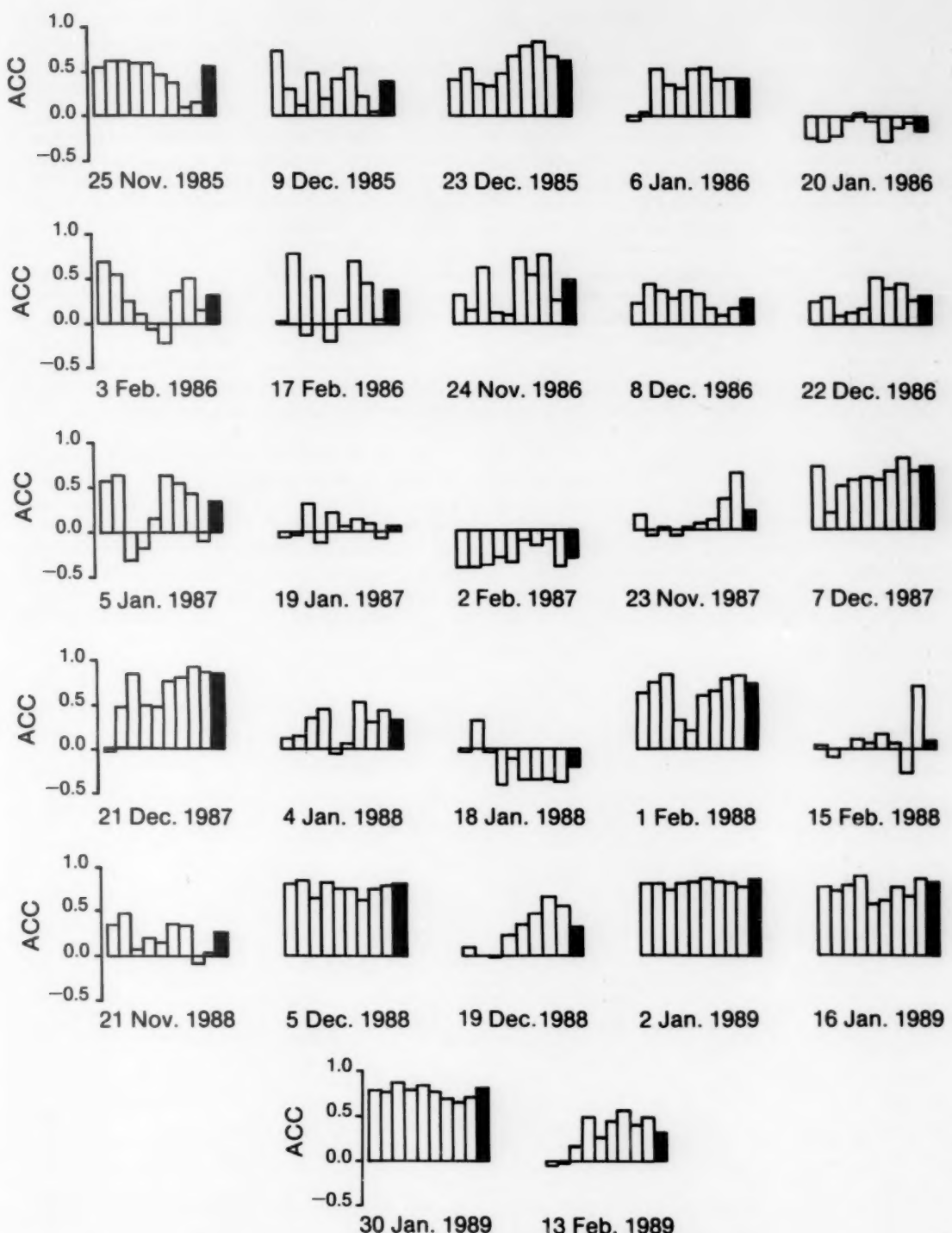


Figure 5. Histograms of anomaly correlation coefficients (ACC) across the individual ensemble members for the 27 winter ensembles at days 6–15 for MSLP over the North Atlantic and Europe. The solid bar is the ensemble mean and the individual members are plotted in order of increasing analysis time from left to right.

poorly, with no difference in skill between the two when averaged over all seasons. On a seasonal basis the ensemble mean is an improvement over MVA in pre-summer (May/June) and more notably in pre-winter (November/December). However, given the small number of samples in any one season and ACC close to their saturation values (noise level) these differences cannot be considered statistically significant.

One question not addressed is whether the additional skill in the ensemble MSLP fields at days 6–15 is actually communicated to the forecasts of temperature and rainfall via the regression equations. The 1-year running-mean skill for the issued temperature forecasts using the Folland–Painting score (Folland *et al.* 1986) from December 1963 to December 1989 is shown in Fig. 6. The skill score is calculated by classifying the forecast and observed temperatures/rainfall into equi-probable quints/terces derived from the climate distribution for 1951–80, and then scoring according to how close the forecast and observed quints/terces are to one another. A score of 100% represents a perfect forecast, 0% a random forecast and –100% a mirror image forecast of the observed state (e.g. forecasting extreme warm conditions when extreme cold ones occurred). The time-series may be tentative evidence of the influence of the dynamical forecasts, with the skill of the recently issued forecasts at an all-time high of 40%.

Although the skill of persistence is almost as high it is noticeable that in past persistent periods issued forecasts have not been as skilful.

4. Prediction of forecast skill

The second and perhaps more important objective of the ensemble forecast is to provide an estimate of the forecast skill at the time the forecast is issued. This opinion is voiced most strongly by Tennekes *et al.* (1986), who state that 'forecast skill ought to be treated as one of the major forecast variables'. In theory this is provided by the ensemble spread. As with skill, a number of spread measures can be calculated. The one used is analogous to anomaly correlation, and is formed as the average anomaly correlation between the individual ensemble members and the ensemble mean. This measure is termed forecast agreement (Kistler *et al.* 1988), and has a value close to one when the agreement is good.

Table II gives the correlation coefficients between ensemble-mean anomaly correlation and ensemble forecast agreement for the three forecast periods and for each season. At days 1–5 for the North Atlantic and Europe the correlation is generally high, the exception being the summer forecasts. However, by days 6–15 the correlation between spread and skill has dropped dramatically, becoming negative for summer and

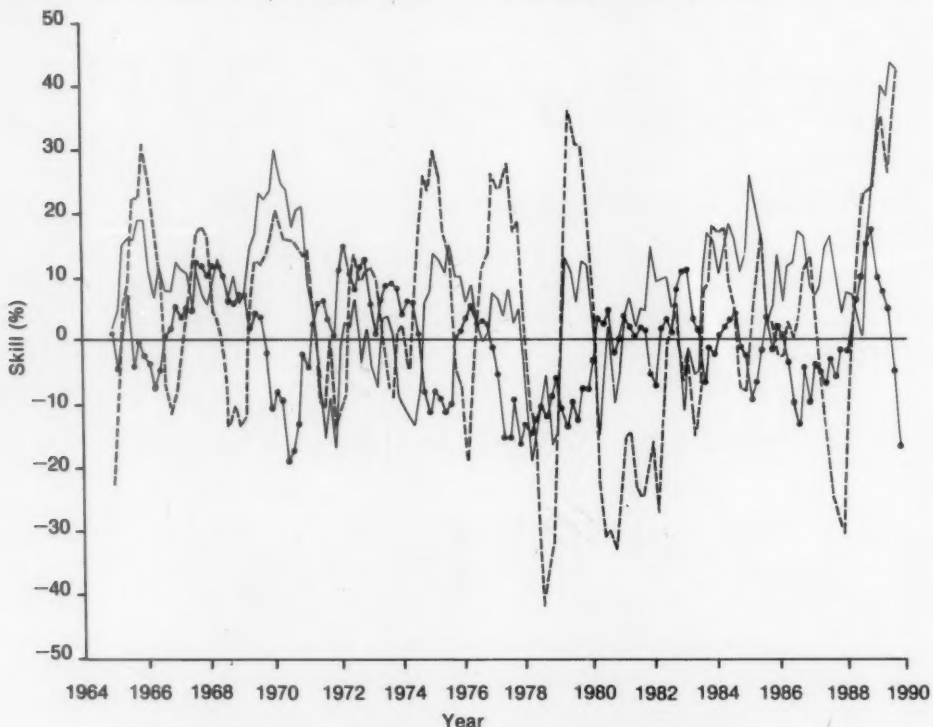


Figure 6. One-year running-mean skill for temperature quints, based on the Folland–Painting score, plotted every 2 months from December 1963 to December 1989. The continuous line represents the issued forecast, the dashed line the persistence and the continuous line with dots the climatology.

autumn, and just above zero for the winter ensembles. For the spring ensembles the correlation remains remarkably high. The correlations are improved at days 6–15 if one considers the northern hemisphere, with all seasons displaying positive correlations and spring once again producing a high correlation coefficient. However, even this fairly large database still suffers from considerable sampling fluctuations.

The scatter diagram between ACC and forecast agreement for the winter ensembles is presented in Fig. 7. The linear relationship between the two is clear at days 1–5, but the scatter is much larger at days 6–15. Closer inspection reveals that there is some variation in the spread–skill relationship between years. For 1985/86 there is a clear linear relationship for six of the seven forecasts, with one forecast for 20 January 1986 (marked A) showing good agreement when the skill was poor. Similarly 1988/89 has five out of seven forecasts in which the forecast agreement gave the correct indication as to the nature of the skill. However, by the same token the relationships for the other two winters are very poor

with 1987/88 showing little variation in its values of forecast agreement, but large variations in the skill of the ensemble forecasts.

The cases where the skill is poor but all the ensemble members are in agreement are characterized by low frequency transitions which occurred in the real atmosphere but were missed by all the ensemble members. The case of 20 January 1986 was a transition from a zonal flow in January 1986 to a blocked flow in February 1986, which none of the members forecast. Use of the alternative measures of root-mean-square (r.m.s.) error and r.m.s. spread (ensemble standard deviation) in general produce even worse spread–skill correlations. However because the r.m.s. error is not bounded, cases such as 20 January 1986 have a much larger impact on the correlation. In this case the r.m.s. error was almost five times the size of the r.m.s. spread.

It is interesting that the four cases with the lowest agreement or highest spread all began from initial conditions which were blocked in the Atlantic sector, and three of the same four cases also produced the

Table II. Correlations between ensemble-mean anomaly correlation and ensemble forecast agreement for the mean-sea-level pressure field over the North Atlantic and Europe (NA) and the northern hemisphere (NH) for three forecast periods; days 1–5, 6–15 and 16–30.

Season	Number of ensembles	Forecast period					
		Days 1–5		6–15		16–30	
		NA	NH	NA	NH	NA	NH
Winter	27	0.83	0.25	0.11	0.28	0.16	0.16
Spring	12	0.81	0.71	0.67	0.73	0.08	0.02
Summer	14	0.20	0.71	-0.52	0.02	-0.35	0.52
Autumn	12	0.58	0.72	-0.16	0.35	0.32	-0.60

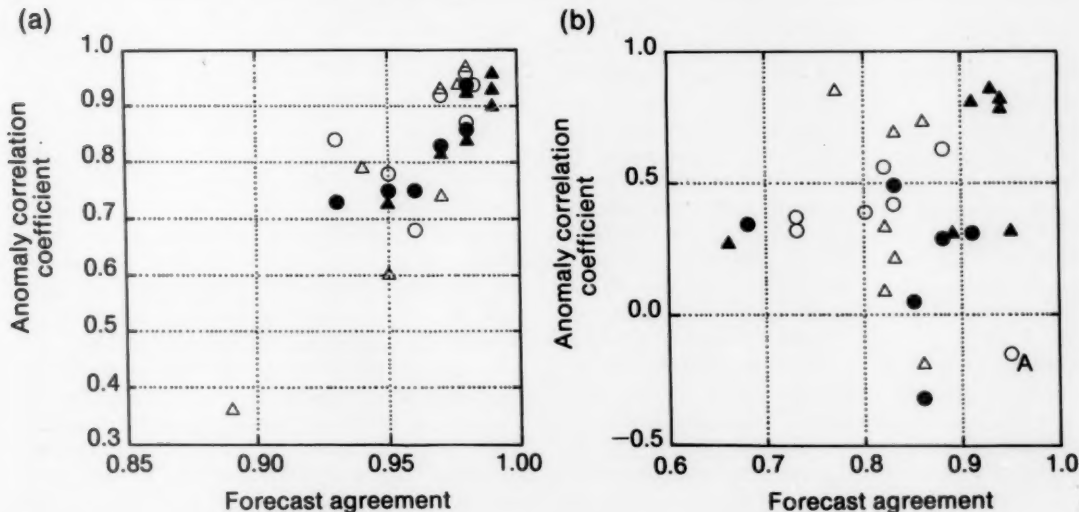


Figure 7. (a) Scatter plot of ensemble-mean anomaly correlation coefficients versus forecast agreement for 27 winter ensembles for MSLP over the North Atlantic and Europe at days 1–5. (b) As (a) but for days 6–15. The winters represented are 1985/86 (open circle), 1986/87 (solid circle), 1987/88 (open triangle) and 1988/89 (solid triangle). For explanation of the plot marked A see text.

highest r.m.s. spreads in the sample. More fruitful results may be gained from considering the dispersion of ensembles in terms of more advanced diagnostics such as the phase-space trajectories used by Brankovic *et al.* (1990), which are able to give information on the temporal evolution of the ensemble probability distribution. This is particularly true if the ensembles exhibit clustering, in which case conventional spread measures may have little meaning.

5. A case-study

The block which formed in February 1986 was the subject of a detailed diagnostic investigation by Hoskins and Sardeshmukh (1987). They concluded that important ingredients for the changes between January and February were the differences in fluxes of heat and momentum due to synoptic weather systems, but that a possible catalyst for the block could have been the anomalous diabatic forcing in the Caribbean region, which may in its turn have been a response to changes in SSTs in this region, or a planetary-scale response to a 30–60 day event which occurred in the tropical west Pacific. This block was also discussed by Folland and Woodcock (1986) in the context of the MVA forecast, as they were able to correctly forecast the persistence of the block for the whole of February, and by Brankovic *et al.* (1990), whose LAF ensemble initialized on 19 January 1986 also failed to capture the transition from zonal to blocked flow. In subsequent experiments Brankovic *et al.* were able to produce a slightly improved forecast by removing the influence of the tropical systematic errors in their model.

As mentioned above, the ensemble initialized on 20 January 1986 failed to capture the transition from zonal to blocked flow. Fig. 8 shows the MSLP fields for the ensemble over the period 31 January–4 February, corresponding to days 11–15 of the forecast. Clearly none of the members has reproduced the blocking signature present in the analysis. The ensemble run from 14 days previously and initialized on 6 January 1986 is shown in Fig. 9, over the verifying period of 1–5 February, corresponding to days 26–30 of the ensemble forecast. At least two of the members from this ensemble have produced a blocking signature. The ODF from 00 UTC on 6 January 1986 has a blocking anticyclone over Denmark, and something of the easterly flow which is present in the verifying analysis that made this February one of the coldest on record. Even more remarkable is the member from 00 UTC on 5 January 1986; this has captured all of the major features, including the cut-off low and large block east of Scandinavia. Although it cannot be ruled out that the similarity is a random event, it must be remembered that such a pattern represents a large departure from the model's own climatology. Indeed the temporal evolution over the previous two pentads shows that the transition was accurately forecast (Fig. 10)

Whilst the forecast from 00 UTC on 5 January 1986 is not typical it does raise a number of important points. Firstly the model is able to produce dynamical structures which resemble blocks in the real atmosphere, as well as the processes which can initiate such low frequency transitions. However, it does so infrequently, and in common with other dynamical models usually produces blocks which have insufficient amplitude and are too short-lived (Tibaldi and Molteni 1990). The ability of dynamical models to capture such low-frequency transitions is the key to successful dynamical extended-range forecasting, and this failing is the major drawback to realizing the potential of the ensemble forecast technique. More studies such as those of Hoskins and Sardeshmukh (1987) into the relevant mechanisms in such cases are necessary if improvements to dynamical models and ultimately progress in dynamical extended-range forecasting are to be made.

Hope for the future is that improvements in model formulation will lead to a more realistic representation of low-frequency variability, at least to the extent that when a block occurs in the real atmosphere a certain proportion of the ensemble members capture it. This would lead to the more probabilistic framework discussed in section 2.1.

6. Conclusions

Real-time, lagged-average forecast ensembles are now a regular feature of the long-range forecasts at the Meteorological Office, and are the dominant component at least out to 15 days. The superiority of the dynamical forecasts in this time range over the statistical techniques has been clearly demonstrated, and the ensemble mean proves to be the best dynamical forecast beyond days 1–5 when the individual ensemble members themselves possess some predictability. At days 16–30 the levels of skill are on average low and very variable, and the product provided by the ensemble forecasts is in this sense a marginal one.

There is, on average, a small positive correlation between the skill and the spread, and this may prove only marginally useful in a practical sense. The theoretical relationship between the spread and skill is undoubtedly destroyed by the growth of systematic deficiencies in the model's climate at medium and extended range. This manifests itself most clearly as an inability of the model to undergo major regime transitions with sufficient frequency beyond days 1–5, an example of which was the ensemble from 20 January 1986. The ensemble member from 00 UTC on 5 January 1986 was one of the rare occasions when the model was able to forecast a major transition from zonal to blocked flow. Such variations in predictability, and their sensitivity to initial conditions and model formulation, must be understood if progress is to be made in forecasting for the extended range. These questions will be addressed with the future generation of dynamical models.

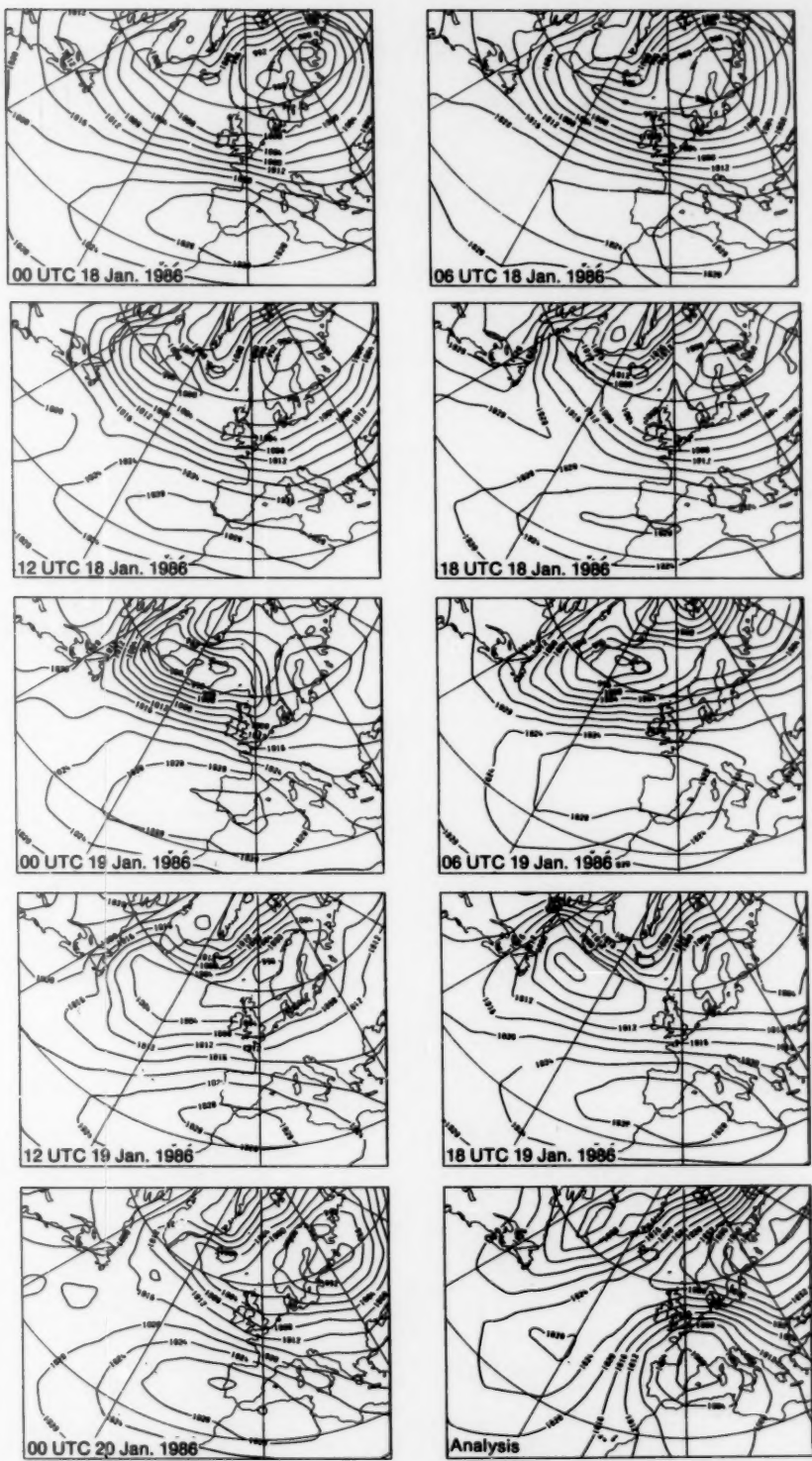


Figure 8. MSLP fields for the individual members of the ensemble initialized on 20 January 1986 and the verifying analysis, for the period 31 January to 4 February, which corresponds to days 11–15 of the ensemble forecast.

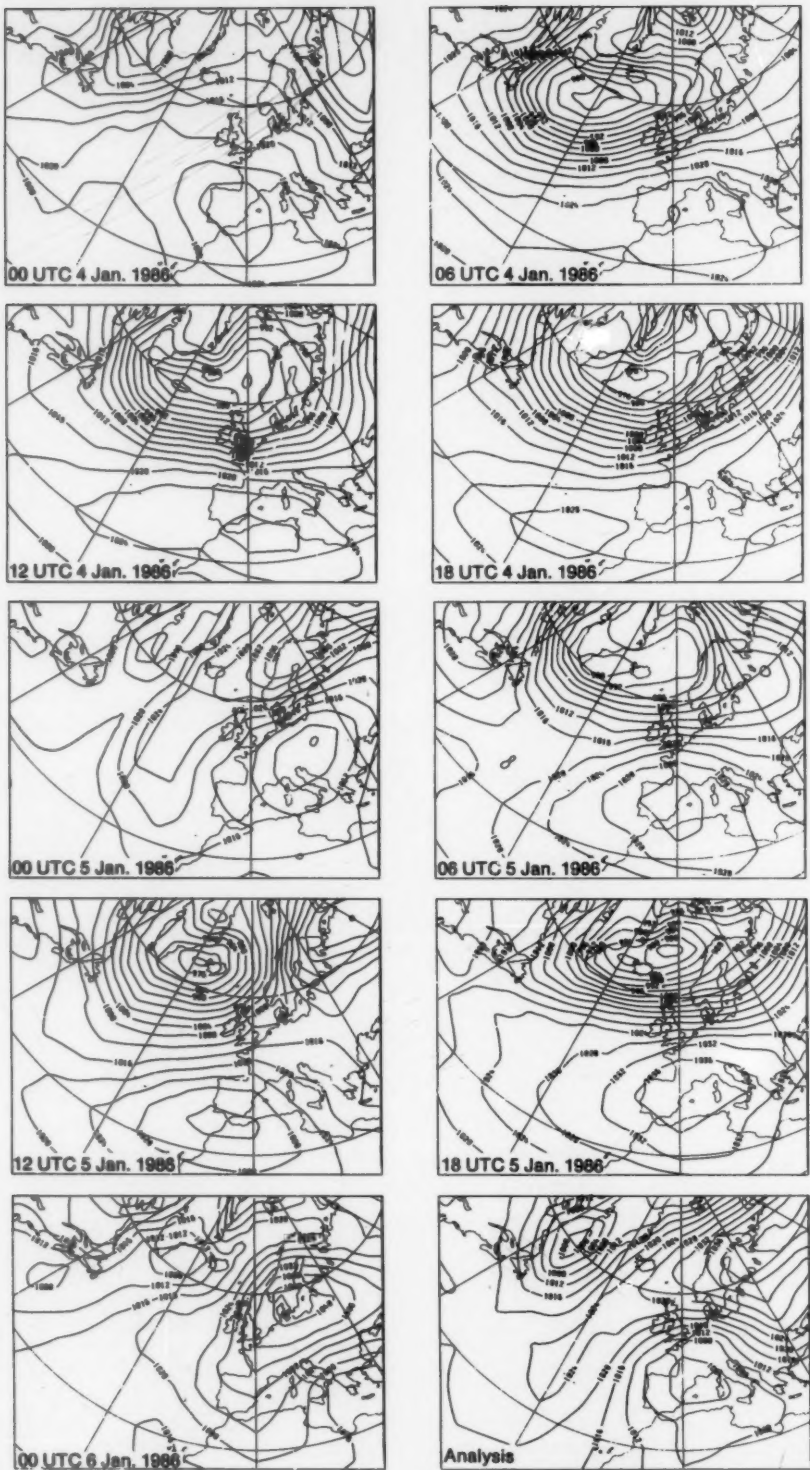


Figure 9. As Fig. 8 but for the ensemble initialized on 6 January 1986. The verification period (1–5 February) corresponds to days 26–30 of the ensemble forecast.

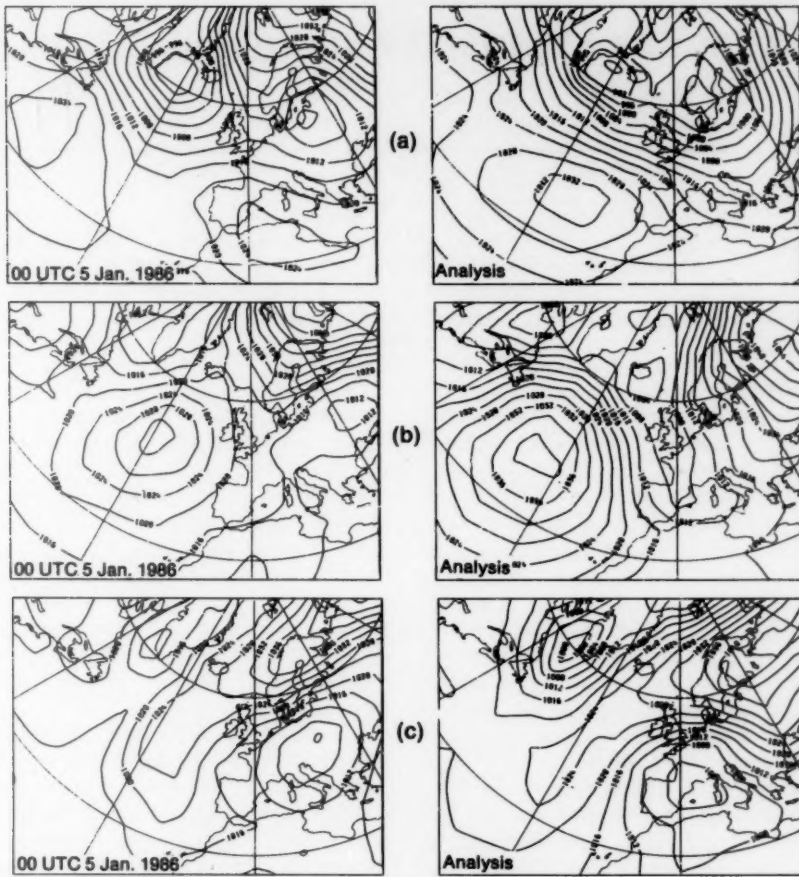


Figure 10. Evolution of the MSLP for the ensemble member initialized at 00 UTC on 5 January 1986 and verifying analysis for (a) days 16–20, (b) days 21–25 and (c) days 26–30 of the ensemble forecast period.

References

- Bell, R.S. and Dickinson, A., 1987: The Meteorological Office operational numerical weather prediction system. *Sci Pap. Meteorol Off*, No.41.
- Brankovic, C., Palmer, T.N., Molteni, F., Tibaldi, S. and Cubasch, U., (1990): Extended-range predictions with ECMWF models. III. Time lagged ensemble forecasting. To appear in *QJR Meteorol Soc*.
- Déqué, M., 1988: The probabilistic formulation: A way to deal with ensemble forecasts. *Ann Geophys*, **6**, 217–223.
- Folland, C.K. and Woodcock, A., 1986: Experimental monthly long-range forecasts for the United Kingdom. Part I. Description of the forecasting system. *Meteorol Mag*, **115**, 301–318.
- Folland, C.K., Woodcock, A. and Varah, L.D., 1986: Experimental monthly long-range forecasts for the United Kingdom. Part III. Skill of the monthly forecasts. *Meteorol Mag*, **115**, 377–395.
- Gilchrist, A., 1986: Long-range forecasting. *QJR Meteorol Soc*, **112**, 567–592.
- Hoffman, R.N. and Kalnay, E., 1983: Lagged average forecasting, an alternative to Monte Carlo forecasting. *Tellus*, **35A**, 100–118.
- Hoskins, B.J. and Sardeshmukh, P.D., 1987: A diagnostic study of the dynamics of the northern hemisphere winter of 1985–86. *QJR Meteorol Soc*, **113**, 759–778.
- Kistler, R., Kalnay, E. and Tracton, M.S., 1988: Forecast agreement, persistence and skill. In Eighth Conference on Numerical Weather Prediction, Baltimore, Maryland, 22–26 February 1988. Boston, American Meteorological Society.
- Leith, C.E., 1974: Theoretical skill of Monte Carlo forecasts. *Mon Weather Rev*, **102**, 409–418.
- Lorenz, E.N., 1982: Atmospheric predictability experiments with a large numerical model. *Tellus*, **34A**, 505–513.
- Maryon, R.H. and Storey, A.M., 1985: A multivariate statistical model for forecasting anomalies of half-monthly mean surface pressure. *J Climatol*, **5**, 561–578.
- Miyakoda, K., Hembree, G.D., Strickler, R.F. and Shulman, I., 1972: Cumulative results of extended forecast experiments. I: Model performance for winter cases. *Mon Weather Rev*, **100**, 836–855.
- Murphy, J.M., 1988: The impact of ensemble forecasts on predictability. *QJR Meteorol Soc*, **114**, 463–493.
- , 1990: Assessment of the practical utility of extended-range ensemble forecasts. *QJR Meteorol Soc*, **116**, 89–125.
- Murphy, J.M. and Palmer, T.N., 1986: Experimental monthly long-range forecasts for the United Kingdom. Part II. A real-time long-range forecast by an ensemble of numerical integrations. *Meteorol Mag*, **115**, 337–349.
- Northcott, G.P., 1989: The winter of 1988/89 in the United Kingdom. *Meteorol Mag*, **118**, 265–267.
- Sutera, A., 1986: Probability density distribution of large-scale atmospheric flow. *Adv Geophys*, **29**, 227–249.
- Tennekes, H., Baede, A.P.M. and Opsteegh, J.D., 1986: Forecasting forecast skill. Proceedings of ECMWF seminar on predictability in the medium and extended range, 17–19 March 1986. Reading, ECMWF. (Copy available in ECMWF, Reading.)
- Tibaldi, S. and Molteni, F., 1990: On the operational predictability of blocking. *Tellus*, **42A**, 343–365.
- Tracton, M.S., Mo, K., Chen, W., Kalnay, E., Kistler, R. and White, G., 1989: Dynamical extended range forecasting (DERF) at the National Meteorological Center. *Mon Weather Rev*, **117**, 1604–1635.

The Interactive Mesoscale Initialization

B.J. Wright and B.W. Golding
Meteorological Office, Bracknell

Summary

The Interactive Mesoscale Initialization (IMI) has been developed to prepare the initial fields for the Meteorological Office mesoscale model. In addition to surface observations, use is made of satellite and radar imagery. Human analysts monitor the initialization procedure, and can incorporate their own knowledge of the situation. Subjective assessment of several cases demonstrates that use of the IMI can lead to improved forecasts.

1. Introduction

The Meteorological Office mesoscale model is used routinely to predict the weather over the British Isles on a 15 km grid. Synoptic-scale development is largely controlled by the time-dependent boundary conditions. However, the mesoscale evolution is sensitive to the initial conditions within the domain, and especially to the humidity distribution. One of the main problems in attempting to specify these initial conditions is the lack of data. The surface observing network has at best a resolution of 50 km, with upper-air observing stations being spaced more than 300 km apart. Over the sea areas the problem becomes greater still with only a few ships and oil rigs providing regular observations.

In an attempt to solve this problem, the Interactive Mesoscale Initialization (IMI) has been developed. This provides an environment within which to make the best possible use of all the available data. A broad range of surface observations is incorporated, including cloud reports, visibility and snow depth, with satellite and radar imagery acting as additional data, providing much needed information over sea areas. These data, together with the most recent forecast fields, are used to produce a set of key analyses of surface variables and cloud distribution. The whole system is under the control of human analysts who, in addition to having control over the use of the data, are able to modify the analyses in order to incorporate their extra knowledge of the situation. Conceptual models are used to relate the other model variables to the analysed quantities.

An assessment programme has been carried out, with subjective comparisons being made between the forecasts run from the current objective initialization (OI) and those run from the IMI. Particular attention has been given to cases where the routine forecast (initialized using the OI) was deficient in some way.

After describing the initialization procedures in some detail (section 3), a summary of the results of this assessment is presented in section 4, with a more detailed look at two of the cases of particular interest.

2. Model formulation

The Meteorological Office mesoscale model (Golding 1987, 1990) uses a non-hydrostatic, compressible

formulation of the primitive equations with a semi-implicit finite difference scheme, allowing a forecast time-step of one minute. An Arakawa C grid of 89×91 points covers the British Isles, with a resolution of 15 km, giving good representation of orography (Fig. 1). A model domain of 63×79 points was used for all the case studies except one, which used an enlarged domain of 120×133 points. The vertical coordinate is height above orography, with 16 levels in the vertical, the lowest at 10 m, the highest at 12 010 m, with the level spacing increasing linearly with height from 110 m to 1510 m.

The model has a detailed boundary-layer mixing formulation with turbulent kinetic energy carried as a variable. Cloud water and humidity are predicted separately to give a good representation of cloud, and both grid-scale and convective precipitation processes are modelled. The radiation scheme is also particularly detailed with respect to cloud.

A continuous 3-hour assimilation cycle is run. The observations are analysed using a combination of a 3-hour mesoscale model forecast and fields interpolated from the most recent forecast from the fine-mesh model (the Meteorological Office regional model) as a first guess. This 'hybrid' first guess takes the synoptic-scale component of the upper-air fields from the fine-mesh model, with the short-wave component derived from the mesoscale model forecast. The cloud and surface fields are also taken from the mesoscale model forecast. The analyses are used to modify the other model variables to obtain a consistent set of model fields. The IMI can be used in the place of this objective initialization.

Two 18-hour forecasts are run each day, from midnight and midday. Hourly predictions are obtained of pressure, wind, grid-scale and convective precipitation, cloud cover and base, visibility, temperature and humidity.

Three-hourly boundary conditions are taken from the fine-mesh model — a 15-level sigma coordinate model, with a resolution of about 75 km in the area of interest. Cloud water mixing ratio is not carried as a variable in the fine-mesh model, and so has to be diagnosed from the relative humidity. This, and the interpolation

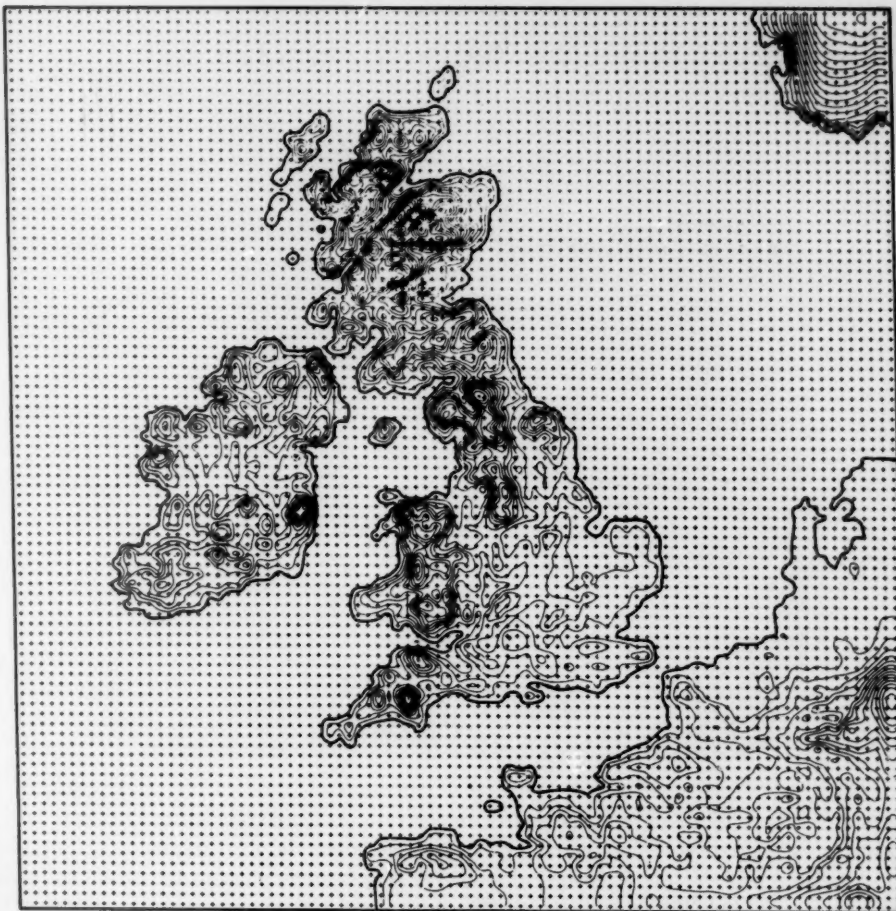


Figure 1. Model domain and orography. The grid points have a 15 km spacing and the contour interval is 50 m. The bold contour is at zero height and indicates the model coastline.

required, can cause undesirable effects close to the boundaries. Because the edges of the model domain are so close to the forecast area the forecast is generally driven by the boundary conditions in the latter stages, although it can develop topographically driven mesoscale features well. But in the first 6–9 hours, and longer in static situations, the initial conditions are very important.

3. Description of initialization schemes

3.1 Interactive Mesoscale Initialization

The IMI is a menu-driven system, controlled by 'mouse' input (and keyboard where required), which is operated by a human analyst on an interactive graphics workstation (Fig. 2). It allows the analyst to monitor the use of surface observations, and satellite and radar imagery, in the production of a set of key analyses of surface variables and the cloud distribution. The analysts are able to modify the data which are used in the analyses and modify the analyses themselves, thus

incorporating their own knowledge of the situation into the final result. Conceptual models are used to make remaining model fields consistent with these analyses.

The analysts have a choice of using the hybrid (see section 2) or a set of fields interpolated from the most recent fine-mesh model forecast as a first guess. The latter is normally selected only if a serious timing error is present in the forecast from the mesoscale model. The first guess is then used as a background field to carry out all the analyses, which are displayed with the observations, for them to check. If they are not satisfied with an analysis, then they have the option of either modifying the observations and reanalysing or modifying the analysis.

The analysts are able to delete, correct or add observations which are then reanalysed using either the first guess or the original analysis as the background field. The use of the original analysis allows the observations to be repeatedly analysed, if necessary, to fit them better. Corrections to the analysis itself can be applied in a broad variety of ways. Areas, lines and



Figure 2. A forecaster in the Central Forecasting Office performing the Interactive Mesoscale Initialization.

points to be altered can be selected on the screen or from a range of values in any of the fields available. In the area selected it is possible to set a value, apply a correction, multiply by a factor, copy values from another field, or smooth the current values with a user-selected smoothing radius. Finally, if the analysts are not satisfied with the result, they have the option of restarting the analysis.

The mean-sea-level (MSL) pressure is analysed first, followed by the 10 m wind components. Before the wind analysis, corrections are made to the first guess to reflect the changes to the geostrophic wind in the pressure analysis. Corrections to the upper-level pressure, potential temperature and wind fields are computed from the pressure and wind analyses. The pressure corrections are calculated from the change in MSL pressure, assuming a slope of one in a hundred normal to the mean MSL pressure gradient, with a linear decrease in magnitude to zero at 8 km. Potential-temperature increments are computed hydrostatically from the pressure corrections at each level. Above 1 km, adjustments to the wind fields are obtained geostrophically from the pressure corrections. Below 1 km a height-dependent, linear combination of the geostrophic correction and the surface correction is used.

A surface precipitation rate analysis is carried out using a FRONTIERS (Brown 1987) radar image as the first guess within the radar coverage area, if an image is available for the correct time. Present weather reports

and hourly accumulations are used to estimate the precipitation rate at the observing stations. These rates are then analysed assuming a small area of influence within the radar domain, but a broader influence outside it. The Meteosat cloud-top-temperature image and sferics reports are usually available to aid the forecaster in verifying the analysis. The distinction between water and ice precipitation is made within the analysis, but is not as yet made use of in the initialization procedure.

The Meteosat cloud-top-temperature image is used to derive an improved first-guess total cloud cover, by assuming that cloud is present whenever the satellite temperature is 10 °C or more colder than the first-guess surface temperature. Because the satellite image is retrieved with a resolution of 7 km, counting the 'cloudy' pixels gives a good estimate of the total cloud cover. The surface reports are then analysed using this improved first guess.

The satellite image is adjusted for surface radiation effects in partially cloudy areas, using the cloud-cover analysis. A cloud-top height field is then derived by using first-guess temperature profiles to assign heights to the satellite cloud-top temperatures. If a satellite image is not available, then the first-guess cloud distribution is used to define the cloud top.

The first-guess cloud base is adjusted to ensure that it is at least 200 m below the cloud top, before it is used as

the background field to analyse the surface observations. If cloud top and cloud base conflict after the cloud-base analysis, then one or the other is modified. Below 8000 ft the cloud base is assumed to be more accurate, so adjustments are made to the cloud top. But, above 8000 ft more faith is placed in the satellite-derived cloud top, so the base is adjusted.

The 8-group cloud reports are analysed using the first-guess cloud distribution, with the cloud-top, base and total-cover analyses acting as constraints. This is carried out by interpolating the first-guess cloud-cover values to the observation points and using them to interpret the 8-groups to give a profile of cloud-cover values at model levels. The values are then analysed level by level.

The cloud and temperature structures may be examined in more detail by selecting up to 20 locations within the model area for which profiles of cloud cover and potential temperature are displayed. Either or both of these profiles may be adjusted if desired, with the temperature corrections and the adjusted cloud-cover values being imposed over an area selected on the screen. To assist the analyst, if a radiosonde ascent is available at the selected location it will also be displayed.

The final four analyses are visibility, lying water (snow depth), screen temperature and dew-point. For the lying-water analysis, state of ground reports of dry, damp, flooded and frost are interpreted quantitatively, and snow depth reports are used directly. The screen-temperature analysis is used to modify the soil, surface and first-level temperatures assuming either a logarithmic or a linear profile depending on the first-guess temperature profile.

The low-level relative humidity, cloud water and the boundary-layer cloud condensation nucleus (CCN) concentration are initialized using the temperature, dew-point and visibility analyses. The humidity mixing ratio is calculated at screen level, and the relative humidity at the lowest level is computed from this by assuming that the humidity mixing ratio remains constant up to 20 m. Where the relative humidity is greater than 99%, or the visibility is less than 1.5 km, cloud water is assumed to be present in the atmosphere and is initialized using an empirical relationship relating it to visibility and CCN concentration (derived from Kunkel 1984):

$$M = \frac{0.03058}{[\text{visibility} \times \{\log_{10}(C_0) + 0.25\}]^{3/2}}$$

where M is the cloud water mixing ratio and C_0 is the first-guess CCN concentration. The relative humidity is also increased to 100% and 8 oktas cloud is set. Elsewhere, the visibility is assumed to depend only on the humidity and the aerosol content. The analysed visibility and relative humidity are used to diagnose the boundary-layer CCN concentration, using an empirical relationship derived from Hänel (1987) and Kunkel (1984):

$$C = \frac{-109732 \times \log_{10}(0.01 \times RH)}{[\text{visibility} \times \{\log_{10}(C_0) + 0.25\}]^{3/2}}$$

where C is the diagnosed CCN concentration, C_0 is the first-guess CCN concentration, and RH is the relative humidity. The cloud-water mixing ratio and the cloud cover are set to zero. The resulting field of C is inherently rough, so it is constrained to be between 20 and 500 cm⁻³ and smoothed.

The upper-level humidity distribution is adjusted to be consistent with the analysed cloud cover, using a simplified form of the equations which are used in the forecast model. Empirical relationships are used to initialize the cloud water/ice profiles consistent with the analysed cloud and precipitation. A single-column version of the model precipitation scheme is used to adjust the cloud water/ice profile iteratively and so produce the analysed precipitation rate at the surface for each grid point.

After the surface temperature has been initialized, it is possible for the analyst to modify the field either by hand or by copying in a sea surface temperature field which has been generated using successive infra-red Meteosat images over the period of a week.

Temperature profiles are adjusted from the lowest level upwards to spread the influence of the surface observations and to enforce stability where no cloud is present. The temperature is adjusted to be stable, using the modified temperature from the level below, and assuming a cloud-fraction dependent, linear combination of the saturated adiabatic lapse rate and the dry adiabatic lapse rate. Immediately above the cloud top, the temperature is adjusted to be stable to air parcels following a saturated adiabat from anywhere within the cloud deck. This allows convective instability within the cloud itself, in a way that is consistent with the forecast-model turbulence scheme, but does not allow instability in the clear air. If necessary, where excess stability is present, it may be eroded in order to minimize deviations from the mean temperature in the first guess. The temperature stability adjustment has been added in an attempt to limit excessive convection which often occurs in the early stages of the forecast.

The divergence profile is adjusted to give zero vertical velocity at the upper boundary. A single-column version of the model precipitation scheme is also used to calculate the height-dependent precipitation rate using the initialized cloud-water profile. Where precipitation is being produced, the vertical velocity is reset so as to lift enough saturated air to replace the precipitation falling out of the layer. The cloud top is reinforced by a small negative vertical velocity. Within the lowest kilometre, the vertical velocity is set equal to a height-dependent, exponentially weighted combination of the vertical velocity recalculated from the horizontal winds and the initialized vertical velocity. A heavy smoothing is applied and values are limited, in order to eliminate sudden changes and unreasonably high values. The

divergence structure is adjusted again to be in balance with this final vertical velocity. Finally, the analyst has to make a 'Yes' or 'No' response, either to use the initial fields which have been created by the IMI, or to fall back on the initial fields generated by the OI.

3.2 Objective initialization (OI)

The main differences between the OI and the IMI are the use of radar and satellite imagery and interactive control given to the analyst. In the OI a similar set of key analyses is carried out and a more limited set of conceptual models is used to make the other model variables consistent. Overall a less thorough knowledge of the situation is incorporated into the initial fields.

The hybrid (see section 2) is taken as a first guess, and thus is used as background for the analyses of MSL pressure, wind, precipitation rate, cloud cover, visibility, snow depth, screen temperature and dew-point. The soil, surface and first-level temperatures are adjusted to be consistent with the analysed screen temperature, preserving the initial-model lapse rate. The temperature, relative humidity and winds within the boundary layer (whose depth is diagnosed from the first-guess temperature profile) are adjusted to be consistent with the analysis values. Super adiabatic lapse rates are removed at all levels. No geostrophic adjustment is made to the winds, but the upper-level pressures are recalculated hydrostatically, starting from the analysed MSL pressure.

The first-level relative humidity and cloud-water mixing ratio are diagnosed from the analysed visibility. The surface observations of cloud are used in conjunction with the cloud-cover analysis to generate a three-dimensional cloud analysis, which in turn is used to initialize relative humidity and to obtain a first-guess cloud-water mixing ratio distribution. A single-column version of the model precipitation scheme is used iteratively to adjust the cloud-water mixing ratio until it produces the analysed precipitation rate. The divergence profile is recalculated to give zero vertical velocity at the upper boundary, but no account is taken of precipitation within the vertical-velocity initialization.

4. Case studies

4.1 Summary of results

Forecasts were run for eight cases using initial conditions generated by both the OI and the IMI. Each case was chosen because the routine forecast (initialized using the OI) was deficient in some way. The comparison between the two forecast runs was, in each case, a subjective one, with the type of comparison being dictated by the particular details of the weather which were of interest to the forecaster on that day.

A summary of the cases is given below, with the impact to the forecast of using the IMI referred to as either none (no major differences from the OI forecast), some (some significant improvements to the forecast

and good (some very marked improvements to the forecast). It is worth noting that in none of the cases investigated did the use of the IMI have a negative impact on the forecast.

Case 1. Stratocumulus cloud and fog. Analysis time 1200 UTC on 5 November 1988. Impact - good.

See section 4.2.

Case 2. Rain and snow. Analysis time 1200 UTC on 26 February 1989. Impact - none.

A complex low-pressure system covered the British Isles. Within the north-westerly flow a small low centre formed and swung south-eastwards across Ireland, Wales and southern England, bringing rain across the south of the country, with snow on the northern edge, and triggering some thunderstorms along the south coast. Both of the forecasts failed to maintain the area of precipitation for more than a few hours into the forecast, leaving most of southern England with a dry afternoon.

Case 3. Frontal precipitation. Analysis time 0600 UTC on 15 February 1989. Impact - some.

See section 4.3.

Case 4. Stratocumulus cloud. Analysis time 0000 UTC on 12 December 1988. Impact - good.

An anticyclone was centred over Ireland, with a weak cold front moving south-westwards across England. There was much low cloud associated with the front and the general area of warm, moist air circulating around the high centre. The OI forecast maintained too much cloud over southern England, whereas the IMI forecast developed the observed breaks and so gave much better guidance.

Case 5. Winds. Analysis time 0000 UTC on 5 May 1989. Impact - some.

A generally slack, anticyclonic pressure gradient covered the British Isles. The OI forecast developed unrealistically strong southerly winds in the North Sea, resulting in a spurious trough which propagated slowly eastwards. The winds were much lighter in the IMI forecast, leading to a more realistic evolution.

Case 6. Convection. Analysis time 0000 UTC on 23 May 1989. Impact - none.

Under the influence of anticyclonic conditions, with very warm, moist air feeding northward across the country, a mesoscale convective system (MCS) moved north from France and redeveloped over Hampshire. Both the forecasts totally failed to develop this feature.

Case 7. Convection. Analysis time 0000 UTC on 24 May 1989. Impact - some.

The situation was the same as case 6 except that the MCS developed slightly later in the night. Despite

initially having quite a good representation of the feature the OI forecast failed to maintain it beyond 06 UTC. The IMI forecast did not have the feature particularly well represented at the beginning of the forecast, but did manage to develop and maintain the feature, correctly moving it north-westwards, albeit rather slower than reality.

Case 8 (carried out on the large model area). Depression. Analysis time 0000 UTC on 11 April 1989. Impact - some.

A deep depression was centred to the north-west of Scotland, with a strong south-westerly flow covering the British Isles. A small low ran to the south of the main centre, developing as it moved into Ireland. The OI forecast did not develop the small low properly, instead concentrating on another centre further north, which meant the frontal rain bands were not well predicted. The IMI forecast developed the small low more successfully, resulting in a more realistic rain-band structure. It also correctly had stronger winds in the following westerly flow.

The following two sections take a more detailed look at cases 1 and 3.

4.2 Anticyclonic stratocumulus (5 November 1988)

The use of satellite imagery and manual intervention within the IMI should lead to a better cloud analysis, and thus a better cloud forecast. This is especially true for static situations involving persistent layer-cloud, such as anticyclonic stratocumulus, where the boundary conditions become less crucial. The case investigated here is such a cloud forecast.

On the evening of 5 November 1988, under the influence of anticyclonic conditions (see Fig. 3), fog formed over much of southern England and remained for several days in some parts. The thickness of the fog

experienced in many places may have been a consequence of the large amount of smoke ejected into the air by bonfires on that evening, but the actual distribution of the fog was very much dependent on the low-cloud distribution, as Fig. 4 shows. A good forecast of the movement and development of the stratocumulus cloud present in the high cell circulation was crucial for the prediction of the onset and the distribution of the fog that night. The midday run of the mesoscale model did not produce a very good 18-hour cloud forecast and failed to develop the observed fog, instead keeping

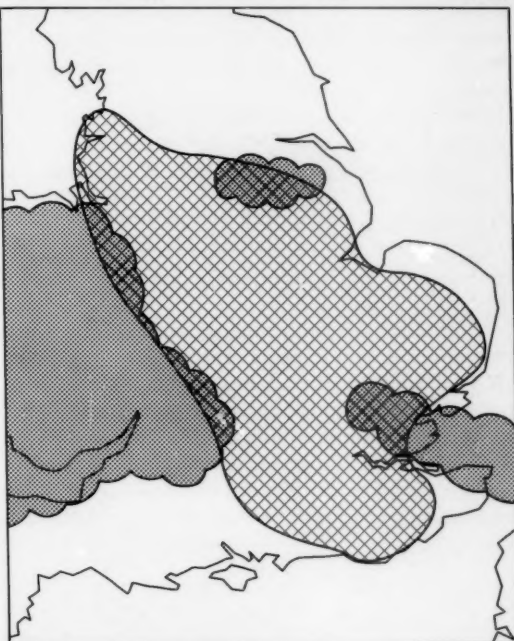


Figure 4. Observed low-cloud areas and fog distribution for 06 UTC on 6 November 1988. Stippling denotes areas with more than 5 oktas low-cloud cover, and hatching denotes areas of less than 100 m visibility.

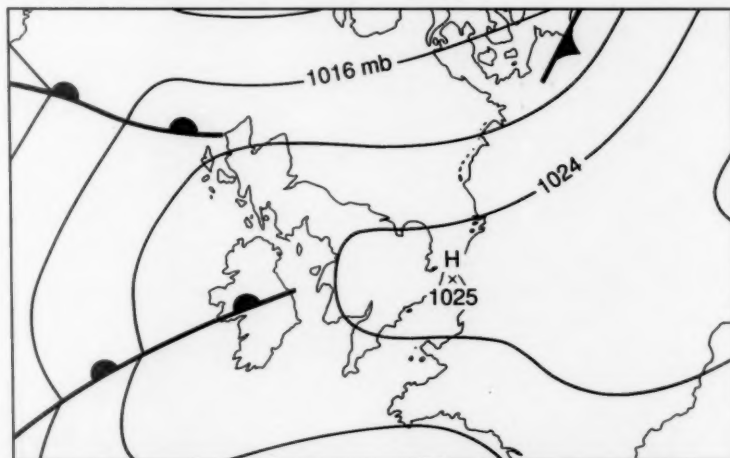


Figure 3. Mean-sea-level pressure analysis and fronts at 06 UTC on 6 November 1988.

visibilities in excess of 20 km. The forecast run from the IMI had a better cloud distribution which was reflected in the lower visibilities produced.

Within the IMI, the Meteosat image was used in both the cloud-cover and the cloud-top analyses. After incorporating the observations, the cloud cover appeared slightly deficient to the north of East Anglia, so 7 oktas cloud was set where the satellite image showed cloud temperatures colder than 0 °C. With very little data present to influence the analysed cloud bases over the sea areas, they appeared to be too high over the North Sea and to the west of Scotland. So, in these areas, the bases were adjusted to agree with the few observations that were available. The resultant cloud analysis produced by the IMI (Fig. 5(a)) has much more low cloud over the sea areas than the objective analysis (Fig. 5(b)), which illustrates the importance of the satellite image over data-sparse areas. Otherwise the two analyses are generally similar over much of the British Isles, except over Wales and the Irish Sea, where the cloud is more broken in the IMI analysis. There is also less high cloud in the IMI analysis and cloud tops over Ireland are higher.

The 18-hour forecast run from the IMI has a cloud sheet covering Wales and just beginning to extend into England, but with the majority of southern England cloud free (Fig. 6(a)), which compares favourably with the observed low-cloud distribution at 06 UTC (Fig. 4). By contrast, the forecast run from the OI has much of southern England under a veil of low cloud, with the only significant breaks being on the south coast and in

Humberside (Fig. 6(b)), this being a very poor reflection of reality. So the incorporation of satellite imagery has had a marked impact on the 18-hour low-cloud forecast.

The forecast visibilities were not as impressive, with the IMI forecast failing to develop the observed fog. But its visibilities were of the order of 4 km over most of southern England, which is a marked improvement on the OI forecast which kept visibilities at over 20 km. The improvement in the visibility forecast is a result of the improved cloud forecast and the higher aerosol concentrations initialized in the visibility analysis. Possible reasons for the failure to forecast the fog are the non-representation of the increase in aerosol concentration which occurred during the evening as a result of the bonfires across the country, and the omission of any interaction between the cloud condensation nucleus concentration (which acts only as a tracer in the forecast) and other model variables.

The use of the satellite imagery within the IMI was reflected in the overall improvement in the forecast. The failure to produce the observed fog is disappointing, but the cloud forecast in itself would have been good guidance to the forecaster trying to predict the fog distribution on the morning of the 6th.

4.3 Frontal precipitation (15 February 1989)

Radar imagery is currently the only available source of data that captures the mesoscale detail present within frontal rain bands. Thus the incorporation of these data within the IMI should lead to a better precipitation analysis, which, when used in conjunction with the

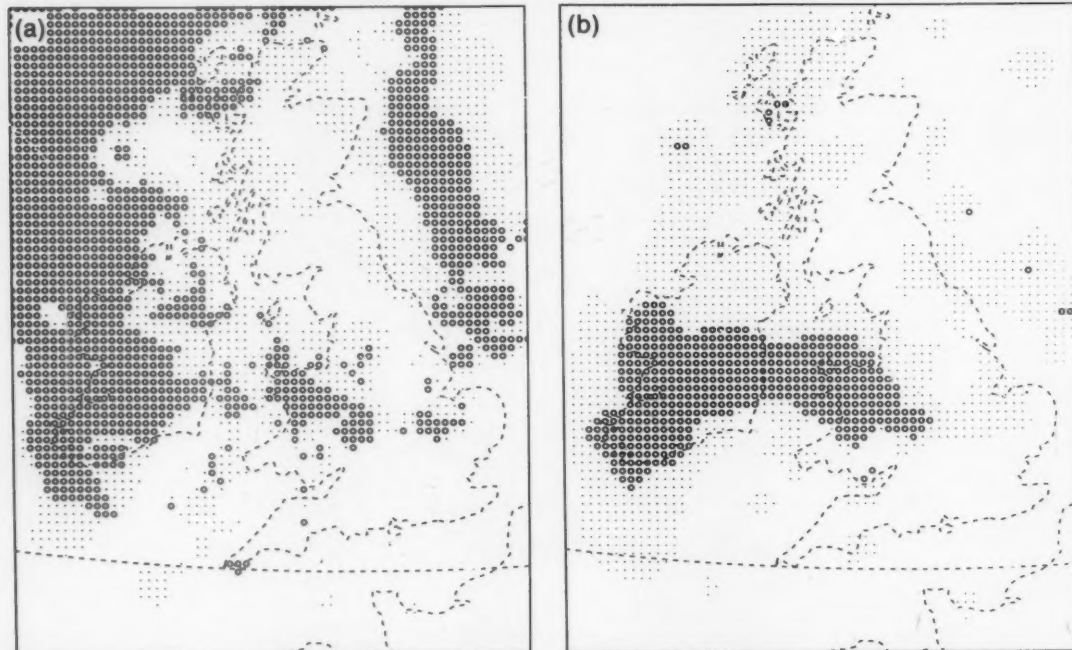


Figure 5. Model analyses of low-cloud cover for 12 UTC on 5 November 1988 for (a) the IMI analysis, and (b) the objective analysis. Cloud amounts are shown as dots, > 4 oktas, or circles, > 7.5 oktas.

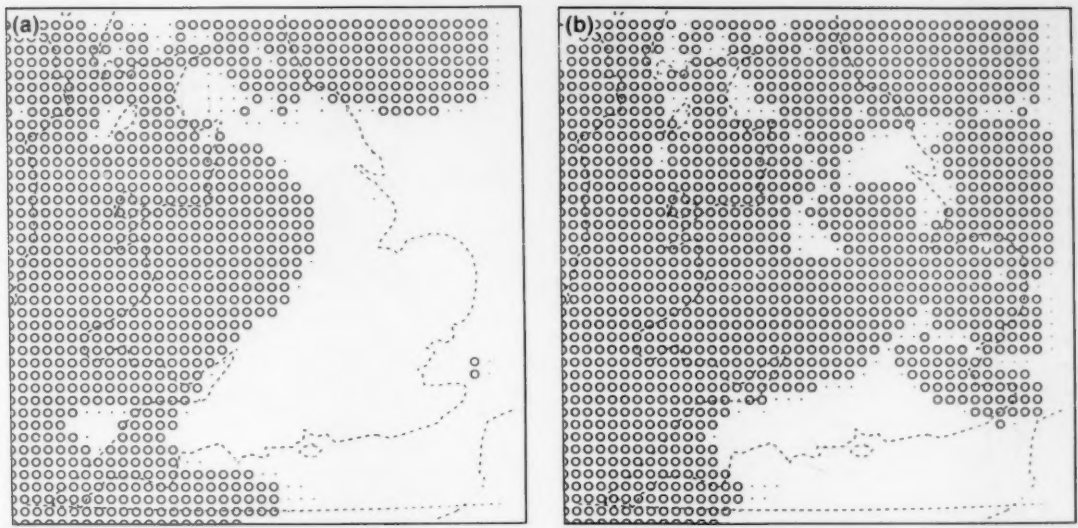


Figure 6. Eighteen-hour forecast low-cloud cover for 06 UTC on 6 November 1988 for (a) the IMI forecast, and (b) the objective forecast. Cloud amounts are shown as dots, > 4 oktas, or circles, > 7.5 oktas.

satellite-derived, three-dimensional cloud analysis in the initialization of the cloud water and the vertical velocity, should generate and maintain a realistic frontal structure. This case investigates the impact of the IMI in the forecasting of a cold front.

On 15 February 1989 an active cold front passed south-eastwards across the British Isles (Fig. 7). Associated with it was an area of heavy rain and a well marked band of line convection (see Fig. 9). Both the midnight and midday runs of the mesoscale model moved the front on too fast, tending to lose the rain to the rear of the front, developing instead a spurious area of rain in the English Channel, well ahead of the front. It was decided to run the mesoscale model, using initial fields generated by both the IMI and the OI at 06 UTC, which was the time when the front first entered the radar domain.

Within the IMI the radar data were incorporated into the precipitation analysis, and produced a good representation of the front over Ireland and northern England. Over the North Sea, where there was no radar coverage and observations were sparse, the front was badly represented. So, within that area, the precipitation was replaced by a rate of 0.4 mm h^{-1} where the Meteosat image showed cloud tops colder than -20°C . The satellite image was also used in generation of the cloud-cover and cloud-top analyses. The front was badly represented in the pressure pattern, so a trough was inserted before the observations were analysed, and was maintained in the analysis. Some spurious fog over northern France was removed. The resultant precipitation analysis produced by the IMI (Fig. 8(a)) had a more continuous band of precipitation than the objective analysis (Fig. 8(b)), with the main area of rain further

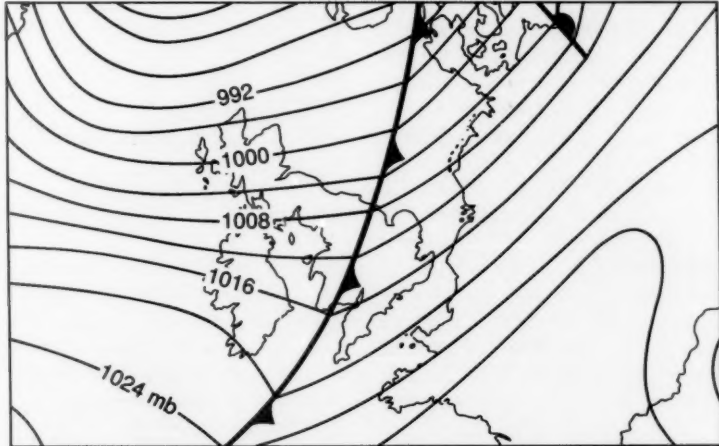


Figure 7. Mean-sea-level pressure analysis and fronts at 12 UTC on 15 February 1989.

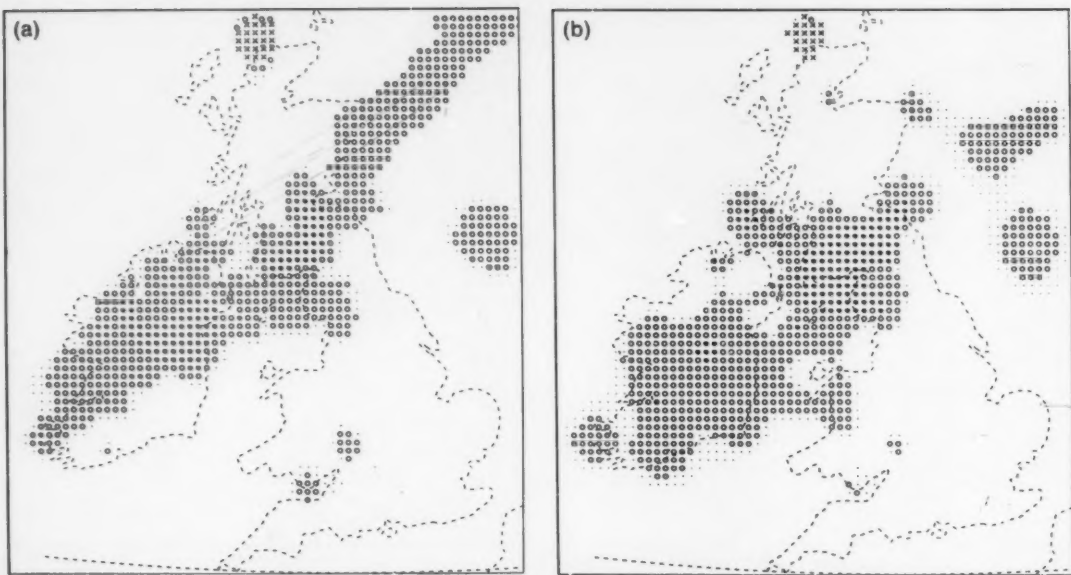


Figure 8. Model analyses of precipitation for 06 UTC on 15 February 1989 for (a) the IMI analysis, and (b) the objective analysis. Dynamic rainfall rates are shown by dots, $>0.05 \text{ mm h}^{-1}$; open circles, $>0.1 \text{ mm h}^{-1}$; solid circles, $>0.5 \text{ mm h}^{-1}$, plus snowfall (rainfall equivalent) by crosses, $>0.05 \text{ mm h}^{-1}$ or asterisks, $>0.5 \text{ mm h}^{-1}$.

north over Ireland, leaving southern Ireland and Wales dry at 06 UTC.

The radar image for 12 UTC (Fig. 9) shows a large area of moderate rain over Wales, with a narrow band of line convection stretching from The Wash through to the Bristol Channel. There are some smaller areas of rain apparent over Cornwall, and there is an area of light rain over south-west and central southern England which does not show up on the radar, but was observed, the area at 12 UTC being shown in Fig. 10.

The 6-hour forecast run from the OI (Fig. 11(b)) has a band of rain which is roughly coincidental with the line convection, but far too wide, with too much rain over East Anglia. It has the main area of rain too far south, over south-west England, where there was only light rain in reality, and much of Wales is completely dry. It has also developed a large area of precipitation over the English Channel, giving southern England and the north coast of France some rain. This area of rain was not supported by observations or radar and appears to be totally spurious.

The forecast run from the IMI (Fig. 11(a)) has a sharper band of quite heavy rain which agrees well with the actual position of the line convection. Like the OI forecast, it has the main area of moderate rain too far south, but does have slightly more rain over Wales. South-east England has been left completely dry which is in accordance with reality, and although there is evidence of the area of spurious rain in the English Channel, it has not been developed to the same extent as in the OI forecast.

Further into the forecast period, both the OI and the IMI forecasts continued to have the rain too far south,

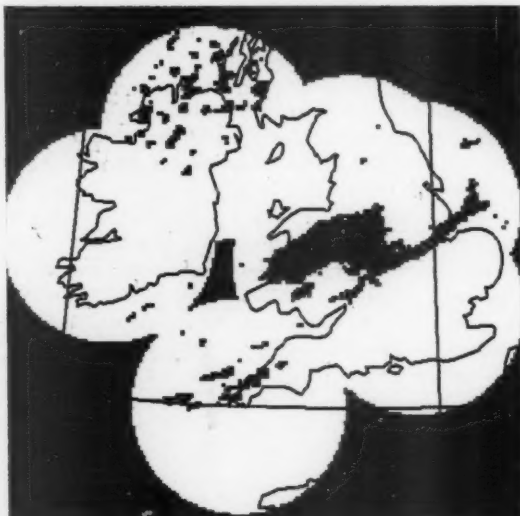


Figure 9. Composite radar image showing areas of precipitation for 12 UTC on 15 February 1989. Within the area of radar coverage the colours blue, green and red denote increasing rates of rainfall.

and developed the spurious rain area over the English Channel. However, the spurious rain was not developed so soon or to the same extent within the IMI forecast as it was within the OI forecast. The IMI forecast also had the convective band slightly further north towards the end of the forecast, giving a better indication of the real distribution of the rain.

Although the use of the satellite and radar data within the framework of the IMI did not totally remove the

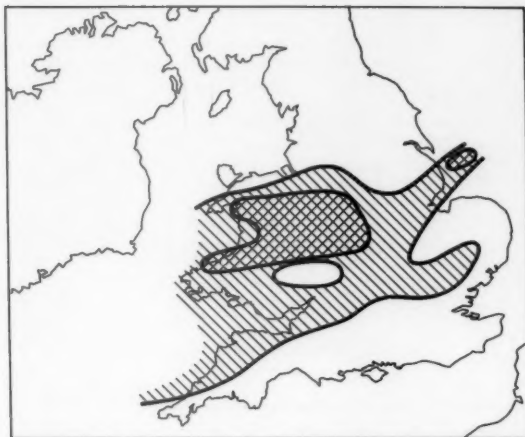


Figure 10. Areas of rain from surface observations for 12 UTC on 15 February 1989. Hatching denotes areas of light rain and cross-hatching areas of moderate or heavy rain.

forecast errors, it did provide some improvements on the OI forecast, especially in the early stages, and would have acted as better guidance to the forecaster attempting to predict the rain areas. The incorrect development of rain in the English Channel may have been a result of erroneous boundary conditions.

5. Conclusions and further work

The eight cases investigated here illustrate that the use of the IMI scheme, incorporating satellite and radar imagery, can have a positive impact on the mesoscale model forecasts.

The most significant improvements occurred in the predicted low-cloud distribution, in static situations such as cases 1 and 4. These cases illustrate that the impact of an improved cloud analysis can last throughout the forecast period. The impact was generally not so long-lived in more mobile situations, such as case 3, with significant improvements tending to last only for the first 6–9 hours. The prolonged impact experienced in case 8 when using a larger domain supports the idea that this limit is due to the influence of the boundary conditions. In cases 2 and 6 the use of the IMI appeared to have no effect on the forecasts, which in both cases, failed to develop a small-scale feature which had a significant effect on the weather. One possible explanation is that the observed feature was not initialized properly, due either to lack of information or shortcomings in the methods used to initialize the upper-air fields.

Future improvements which may reduce the problems are likely to come from increasing the model domain, the use of more conceptual models and the utilization of other sources of data as they become available. Further comparisons between the OI and the IMI could usefully be carried out in several ways.

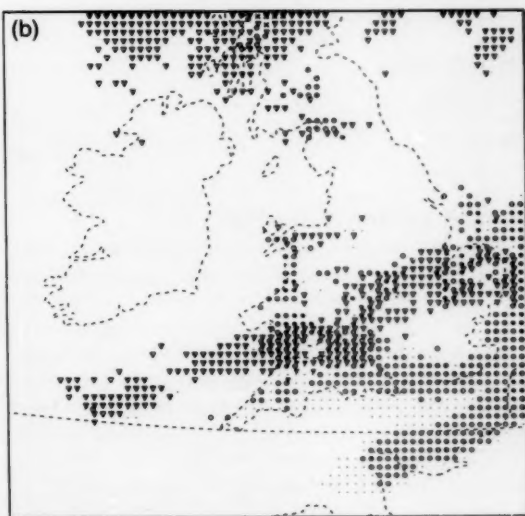
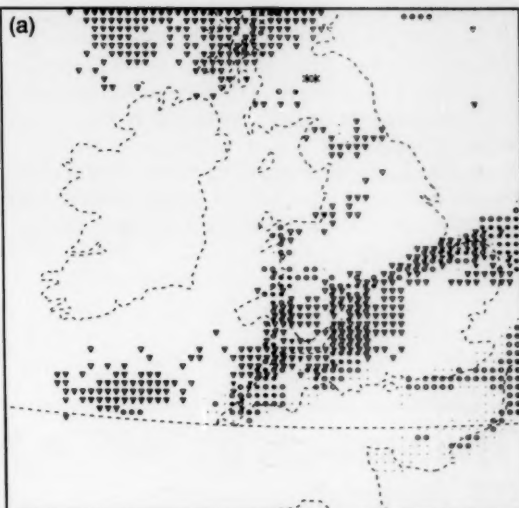


Figure 11. Six-hour forecast precipitation for 12 UTC on 15 February 1989 for (a) the IMI forecast, and (b) the objective forecast. Dynamic rainfall rates are as in Fig. 8 with the addition of convective rainfall denoted by open triangles, $>0.4 \text{ mm h}^{-1}$ or solid triangles, $>2 \text{ mm h}^{-1}$.

In all the cases investigated here, the routine forecast (initialized using the OI) has been deficient in some way, thus leaving plenty of room for improvement. To obtain a more balanced view of the effect that the use of the IMI has on the forecast, it would be beneficial to run some comparisons on cases where the use of the OI has resulted in a good forecast, to see if the IMI provides further improvements to the forecast, has no impact or possibly degrades it.

Another factor in this assessment is that the cases shown here have all been carried out in a research environment, away from the pressures and time constraints experienced by a forecaster in the Central

Forecasting Office (CFO). The next logical stage in the assessment of the IMI, would be to compare forecasts initialized by forecasters in CFO using the IMI with those initialized using the OI. This would provide a much better insight into the improvements that could be obtained by using the IMI operationally.

Since the mesoscale model has a continuous assimilation cycle, it would also be useful to compare forecasts when the OI and the IMI had been used on more than one assimilation cycle.

References

- Brown, R., 1987: The use of imagery in the FRONTIERS precipitation nowcasting system. In Proceedings of the workshop on satellite and radar imagery interpretation, Reading, England, 24 July 1987.
- Golding, B.W., 1987: Short-range forecasting over the United Kingdom using a mesoscale forecasting system. In Matsuno T. (Ed.), Short and medium-range numerical weather prediction. Tokyo, Meteorological Society of Japan.
- , 1990: The Meteorological Office mesoscale model. *Meteorol Mag*, 119, 81–96.
- Hanel, G., 1987: The role of the aerosol properties during the condensational stage of cloud: A reinvestigation of the numerics and microphysics. *Contrib to Atmos Phys*, 60, 321–339.
- Kunkel, B.A., 1984: Parameterization of droplet terminal velocity and extinction coefficient in fog models. *J Clim Appl Meteorol*, 23, 34–41.

551.506.1(41-4)

The autumn of 1989 in the United Kingdom

G.P. Northcott

Meteorological Office, Bracknell

Summary

The mild, dry and mainly sunny weather of the summer continued well into the autumn, but with localized thundery outbreaks in September, some windy days in October and widespread fog for a while in November.

1. The autumn as a whole

Over the autumn season mean temperatures were above normal in all areas of the United Kingdom except parts of western Scotland and ranged from 1.4 °C above normal in the area north of London to 0.4 °C below normal on the Isle of Rhum. Rainfall amounts were below normal nearly everywhere with as little as 40% in parts of East Anglia, north-east England and south-east Scotland. However, in parts of South Wales and the west of England amounts were above normal, with about 120% in Hereford and Worcester and north Cornwall. Autumn sunshine totals were high in many inland areas, but rather low in the west, ranging from more than 120% of normal in the north of Scotland to less than 80% of normal in the Isle of Man.

Information about the temperature, rainfall and sunshine during the period from September to November 1989 is given in Fig. 1 and Table I.

2. The individual months

September. Mean monthly temperatures were above normal in England and Wales but near normal in Scotland and Northern Ireland, ranging from 0.5 °C below normal at Abbot'sinch, Strathclyde Region to 2.1 °C above normal at Gatwick, West Sussex. The mean temperature over England and Wales was the highest since 1961, not because daytime temperatures were particularly notable, but rather that night-time temperatures were unusually high. Hampstead, Greater London reported the highest mean maximum since 1964

(19.9 °C), the highest mean minimum since 1961 (12.5 °C), and the highest mean temperature since 1961. Oxford reported the warmest September since 1949 (mean maximum 20.1 °C, mean 15.6 °C, mean minimum 11.9 °C). Northwood reported the highest monthly mean since 1959 and 1961. The temperature of 26.1 °C on the 7th gave Northwood its warmest September day since 1972. Broom's Barn, Suffolk had the highest mean air temperature for 40 years (14.2 °C). Monthly rainfall amounts were below normal nearly everywhere, apart from Kinloss, Grampian Region and northern parts of Devon and Cornwall, where rainfall was just above average, ranging from 101% at St Mawgan, Cornwall to only 11% at Leeming, North Yorkshire. Generally it was the driest September only since 1986. However, many places in eastern England had the driest September since 1969, including Hampstead and Northwood, both in Greater London, and Broom's Barn, Suffolk; Durham and Tynemouth in the north-east had the driest September since 1898. Monthly sunshine totals were above normal in northern and eastern Scotland and north-eastern and central areas of England, and near or below normal elsewhere, ranging from 137% at Lerwick, Shetland to 78% at Marham, Norfolk.

The weather was generally fairly settled, warm and dry, but less sunny in many areas than over the previous months. The period from the 10th to 19th was unsettled, and localized severe thunderstorms between the 10th and 13th caused lightning damage and flooding in the

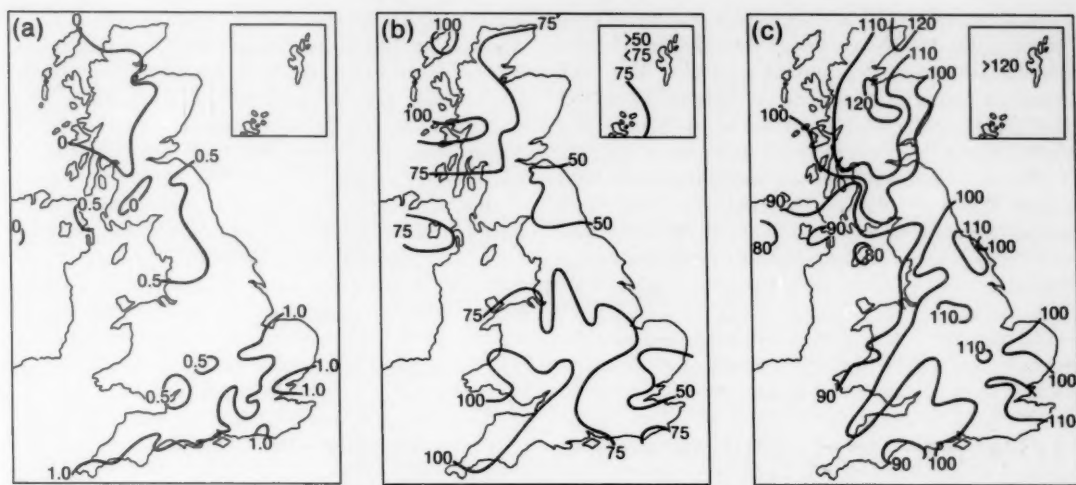


Figure 1. Values of (a) mean temperature difference ($^{\circ}\text{C}$), (b) rainfall percentage and (c) sunshine percentage for autumn, 1989 (September–November) relative to 1951–80 averages.

Table I. District values for the period September–November 1989, relative to 1951–80 averages

District	Mean temperature ($^{\circ}\text{C}$)	Rain-days	Rainfall	Sunshine
	Difference from average		Percentage of average	
Northern Scotland	+0.1	-2	87	118
Eastern Scotland	+0.4	-2	67	112
Eastern and north-east England	+0.8	-3	62	108
East Anglia	+1.0	-2	58	114
Midland counties	+0.8	-3	84	108
South-east and central southern England	+1.1	-3	69	119
Western Scotland	+0.2	-2	80	104
North-west England and North Wales	+0.5	-1	75	100
South-west England and South Wales	+0.8	-2	96	98
Northern Ireland	+0.4	-1	80	88
Scotland	+0.2	-2	81	111
England and Wales	+0.8	-2	77	108

Highest maximum: 27.1°C in Midland counties in September.
Lowest minimum: -8.4°C in western Scotland in November.

south. Areas affected included Kent early on the 10th, Devon and Dorset on the 11th, south Devon and many parts of south-east England on the 12th. Late on the 12th lightning struck and badly damaged houses near Wokingham, Berkshire and at nearby Bracknell. Lightning disrupted ambulance communications at Wokingham for a time. In south and east London flood-water was up to half a metre deep in places. In Kent lightning left thousands of homes in Faversham and some other places without power; near Herne Bay a man was killed by lightning. Among the buildings struck was the Guildhall Museum at Rochester. Many rail services in Kent were disrupted, while rain caused a landslide on the railway at Ruscombe, Berkshire adding to problems caused by signal failures.

October. Mean monthly temperatures were above normal everywhere except northernmost parts of Scotland, ranging from just below normal at Wick,

Highland Region to about 2°C above normal in the London area. Monthly rainfall totals were above normal nearly everywhere apart from parts of eastern and southern Scotland and parts of eastern England and East Anglia, ranging from more than 180% in the southwest Midlands and South Wales to as little as 56% at Lowestoft, Suffolk. Monthly sunshine amounts were about or below normal nearly everywhere. Parts of the east Midlands had between 100% and 123% of normal, while western Wales had only just half the normal.

The weather was relatively quiet at the beginning of the month, then became unsettled with some windy spells; but, between the 14th and 18th it was mainly dry in southern areas of Great Britain. From the 19th it was generally unsettled, with some very wet weather at times. Over Wales the 20th was probably the wettest day since 23 January 1990. Late on the 20th and on the 21st England and Wales became very windy with gusts of more than 50 kn over southern counties of England and

Wales including 63 kn at Sheerness, Kent and 69 kn at Portland Bill, Dorset; two people were killed and several had narrow escapes as gale-force winds and heavy rain disrupted traffic in western areas, brought down trees and caused widespread flooding. Many parts had a period of very heavy rain and strong winds on the 28th, when a very vigorous depression brought gales to many exposed parts of southern England and Wales, with widespread gusts of more than 60 kn in the south-west and a peak of 88 kn at Portland Bill. Further heavy rain affected southern counties overnight on the 30th/31st.

November. Mean monthly temperatures were generally near normal, although some regional differences were evident: values were slightly above average in eastern Scotland, north-east England, Wales and south-west England, while in many central and south-eastern areas of England it was rather cool. Averages ranged from 1.2 °C above normal at Aberdeen, Grampian Region and Falmouth, Cornwall to 0.7 °C below normal at Alice Holt, Hampshire. Monthly rainfall totals were below normal everywhere in the United Kingdom, ranging from as little as 21% at Edinburgh, Lothian Region to 93% in North Wales. Some parts of the Moray Firth area received less than 3 mm of rain during the first 14 days of November, and a few widely scattered locations had no measurable rainfall through-

out the month. Monthly sunshine amounts were above normal nearly everywhere in the United Kingdom except for one or two places in north-west England, the Isle of Man, eastern Scotland and south Devon, and much of Northern Ireland, where it was a little below normal, and ranged from 202% at Folkestone, Kent to about 60% of normal at Omagh, Co. Tyrone. Over much of southern England it was the sunniest November on record. The highest monthly sunshine amount was 147 hours at Folkestone, Kent, the highest November total anywhere in the United Kingdom since sunshine records began. Scotland also had a sunny month, and Edinburgh Royal Observatory recorded 94 hours of sunshine, this value having been exceeded only once (99 hours in 1947) in a record going back to 1901.

The unsettled weather of the last 2 weeks of October continued into the first 10 days or so of November, with some further heavy rain, especially in hilly western areas of Wales and England, although eastern Scotland and coastal areas of north-east England often escaped significant rainfall. Towards mid month settled weather gradually became established over the whole United Kingdom although bringing with it periods of widespread fog, persistent from the 13th to 14th. From the 15th it was mostly dry; most of any rain fell in northern Scotland, or in eastern coastal areas and, until the 22nd, the far south-west of England and Wales.

Notes and news

Water-resource assessment experts meet to develop a strategy for the 1990s

A group of experts met in the Headquarters of the World Meteorological Organization (WMO) from 17 to 19 July to take the first steps towards the preparation of a water-resource assessment strategy for the 1990s. The meeting was sponsored by WMO, the United Nations Educational, Scientific and Cultural Organization (UNESCO), the United Nations Department of Technical Co-operation for Development (UNTCID) and the UN Department of International Economic and Social Affairs (UNDIESA).

In preparation for the meeting, experts/consultants visited countries in different regions of the world. The meeting identified the following problem areas:

- (a) Inability of many nations to assess and manage their water resources wisely, because legislation and/or institutions to carry out the work are lacking.
- (b) Reduction of hydrological networks, as well as the analyses of data from them, by countries suffering from economic difficulties.
- (c) Lack of measurements of ground water and water quality in many regions of the world.
- (d) Inadequate facilities to train and educate technicians and professionals in water-resource assessment in many parts of the world.

The outcome of the meeting and its proposals for future action on national, regional and global scales will be incorporated in an overall assessment report to be prepared by WMO and UNESCO. This report will be submitted to the UN Committee on Natural Resources. It will guide the preparation of plans and projects for water-resource assessments into the next millennium.

European nations check ozone monitoring equipment

More than 40 scientists spent four weeks checking the measuring equipment which provides the world with vital information on the state of the ozone layer. The Ozone Instrument Intercomparison began on 15 July and was scheduled to finish on 10 August. During this period 18 Dobson ozone spectrophotometers, the commonly used ground-based ozone measuring instrument, located in different countries in Europe, were compared. Arrangements were also made for a 2-day seminar on the operation and maintenance of the Brewer ozone spectrophotometer, a newer model first introduced a few years ago.

The current intercomparison, organized by the World Meteorological Organization (WMO), is the third held in Arosa, Switzerland, at the kind invitation of the Swiss Meteorological Institute. Intercomparisons are organized in different regions of the world at three- to four-yearly intervals.

Measurements of the ozone layer began more than 35 years ago. Observations taken with the Dobson equipment are the mainstay of the WMO's Global Ozone Observing System. Today, more than 140 ground-based ozone stations, supplemented by satellites, constitute the backbone of the system. Some 60 WMO Members operate these stations and hundreds of scientists are involved in manning them.

Books received

The listing of books under this heading does not preclude a review in the Meteorological Magazine at a later date.

Principles of air pollution meteorology, by T.J. Lyons and W.D. Scott (London, Belhaven Press, 1990) has an emphasis on industrial emissions but the methods described can be applied generally. The pollutant effects of the principal chemical compounds are also discussed.

The dawn of massively parallel processing in meteorology, edited by G.-R. Hoffman and D.K. Maretis (Berlin, Heidelberg, New York, London, Paris, Tokyo, Hong Kong, Springer-Verlag, 1990) contains the proceedings of the third workshop on this topic held at the European Centre for Medium-range Weather Forecasts (ECMWF). It includes documentation of the advent of such systems and experience in their operational use.

Organic chemistry of the earth's atmosphere, by V.A. Isidorov (Berlin, Heidelberg, New York, London, Paris, Tokyo, Hong Kong, Springer-Verlag, 1990) summarizes the multidisciplinary data on sources and transformations of organic components in the atmosphere. Methods of atmospheric microimpurity analysis and models of time-dimensional distribution are included.

Asymptotic modelling of atmospheric flows, by R. Zeytounian (Berlin, Heidelberg, New York, London, Paris, Tokyo, Hong Kong, Springer-Verlag, 1990) aims to obtain asymptotic models using singular perturbation techniques from fluid mechanics. For meteorological applications filtering to eliminate local interference phenomena is introduced.

Satellite photographs — 13 September 1990 at 1130 UTC

Images from the $6.7\text{ }\mu\text{m}$ water-vapour channel on Meteosat often show distinctive moist (white therefore cold) and dry (black therefore warm) bands that can be related to surface analyses and upper-tropospheric flow patterns. The images are essentially portraying the integrated water-vapour content of a deep layer from 300 mb to near 800 mb, but with a peak contribution from around 400 mb. A real impression of fluid flow can be gained especially when images are viewed on movie-loops. Forecasters can use the images to fine-tune upper-air analyses, with water-vapour images having an important advantage over the $10\text{--}12\text{ }\mu\text{m}$ infra-red channels since zones of high or low moisture have spatial continuity that may not be apparent on the concurrent infra-red image if cloud is not present.

In the water-vapour panorama covering the Atlantic and western Europe in Fig. 1 the boundary between moist and dry air at A is clearly related to the position of the 300 mb jet axis (bold arrowed line). This relation still holds at B although not as clearly defined. The marked dry tongue C south of Iceland is associated with a strong south-westerly jet. The low in this region (the surface analysis is superimposed on the infra-red image in Fig. 2) deepened rapidly during the following 24 hours. The band of moisture associated with the frontal system connected to this low can be traced well south into the subtropics, appearing to be linked with the spiralling outflow from hurricane 'Isidore' (I). Areas of deep convection that have transported moisture up into an otherwise dry upper atmosphere can be seen at D.

A.J. Waters

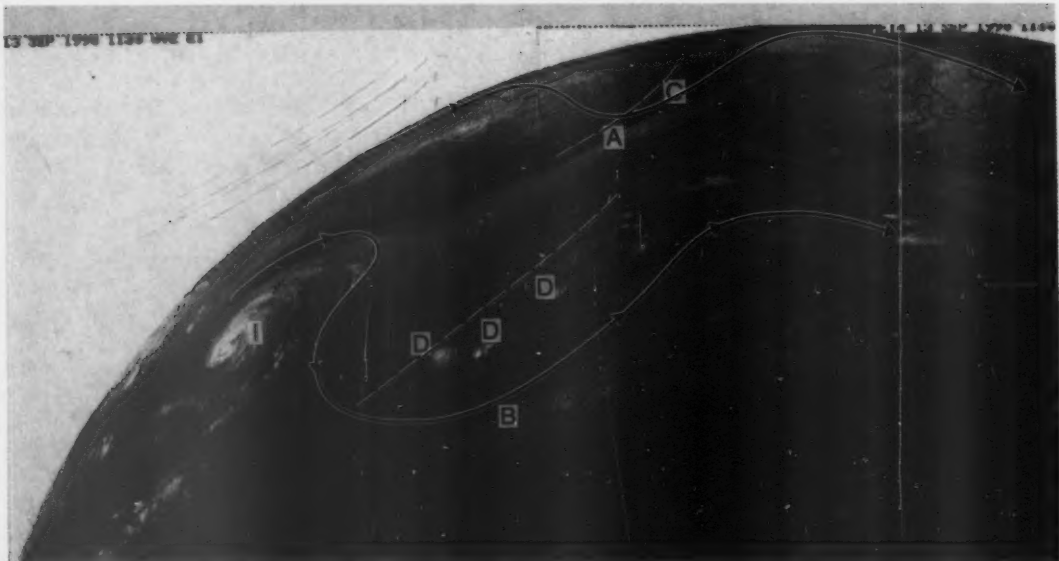


Figure 1. Meteosat water-vapour image at 1130 UTC on 13 September 1990 with the 300 mb jet axis (bold arrowed line) and the 300 mb trough axes (dashed lines) superimposed. Other areas marked are A, the moist-dry boundary layer in the Atlantic; B, as A but near the Azores; C, the dry tongue near Iceland; D, an area of mid-Atlantic deep convection; I, hurricane 'Isidore'.

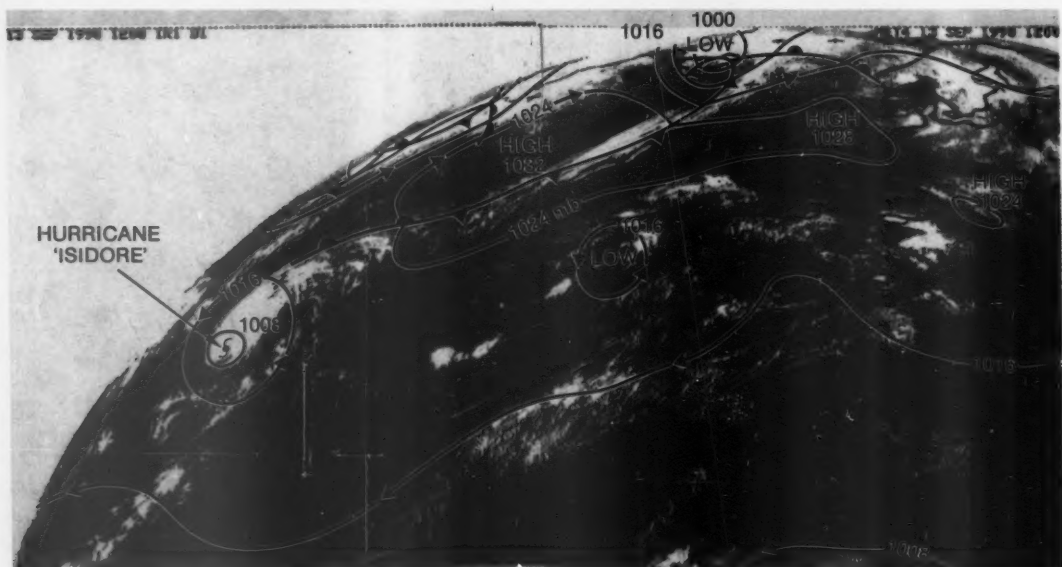


Figure 2. Meteosat infra-red image at 1200 UTC on 13 September 1990 with surface analysis superimposed.

GUIDE TO AUTHORS

Content

Articles on all aspects of meteorology are welcomed, particularly those which describe results of research in applied meteorology or the development of practical forecasting techniques.

Preparation and submission of articles

Articles, which must be in English, should be typed, double-spaced with wide margins, on one side only of A4-size paper. Tables, references and figure captions should be typed separately. Spelling should conform to the preferred spelling in the *Concise Oxford Dictionary* (latest edition). Articles prepared on floppy disk (CompuCorp or IBM-compatible) can be labour-saving, but only a print-out should be submitted in the first instance.

References should be made using the Harvard system (author/date) and full details should be given at the end of the text. If a document is unpublished, details must be given of the library where it may be seen. Documents which are not available to enquirers must not be referred to, except by 'personal communication'.

Tables should be numbered consecutively using roman numerals and provided with headings.

Mathematical notation should be written with extreme care. Particular care should be taken to differentiate between Greek letters and Roman letters for which they could be mistaken. Double subscripts and superscripts should be avoided, as they are difficult to typeset and read. Notation should be kept as simple as possible. Guidance is given in BS 1991: Part 1: 1976, and *Quantities, Units and Symbols* published by the Royal Society. SI units, or units approved by the World Meteorological Organization, should be used.

Articles for publication and all other communications for the Editor should be addressed to: The Chief Executive, Meteorological Office, London Road, Bracknell, Berkshire RG12 2SZ and marked 'For Meteorological Magazine'.

Illustrations

Diagrams must be drawn clearly, preferably in ink, and should not contain any unnecessary or irrelevant details. Explanatory text should not appear on the diagram itself but in the caption. Captions should be typed on a separate sheet of paper and should, as far as possible, explain the meanings of the diagrams without the reader having to refer to the text. The sequential numbering should correspond with the sequential referrals in the text.

Sharp monochrome photographs on glossy paper are preferred; colour prints are acceptable but the use of colour is at the Editor's discretion.

Copyright

Authors should identify the holder of the copyright for their work when they first submit contributions.

Free copies

Three free copies of the magazine (one for a book review) are provided for authors of articles published in it. Separate offprints for each article are not provided.

Contributions: It is requested that all communications to the Editor and books for review be addressed to the Chief Executive, Meteorological Office, London Road, Bracknell, Berkshire RG12 2SZ, and marked 'For Meteorological Magazine'. Contributors are asked to comply with the guidelines given in the *Guide to authors* which appears on the inside back cover. The responsibility for facts and opinions expressed in the signed articles and letters published in *Meteorological Magazine* rests with their respective authors.

Subscriptions: Annual subscription £30.00 including postage; individual copies £2.70 including postage. Applications for postal subscriptions should be made to HMSO, PO Box 276, London SW8 5DT; subscription enquiries 071-873 8499.

Back numbers: Full-size reprints of Vols 1-75 (1866-1940) are available from Johnson Reprint Co. Ltd, 24-28 Oval Road, London NW1 7DX. Complete volumes of *Meteorological Magazine* commencing with volume 54 are available on microfilm from University Microfilms International, 18 Bedford Row, London WC1R 4EJ. Information on microfiche issues is available from Kraus Microfiche, Rte 100, Milwood, NY 10546, USA.

November 1990

Editor: F.E. Underdown

Editorial Board: R.J. Allam, R. Kershaw, W.H. Moores, P.R.S. Salter

Vol. 119

No. 1420

Contents

	Page
Practical extended-range forecasting using dynamical models.	
S.F. Milton	221
The Interactive Mesoscale Initialization. B.J. Wright and B.W. Golding	234
The autumn of 1989 in the United Kingdom. G.P. Northcott	244
 Notes and news	
Water-resource assessment experts meet to develop a strategy for the 1990s	246
European nations check ozone monitoring equipment	246
Books received	247
Satellite photographs — 13 September 1990 at 1130 UTC.	
A.J. Waters	247

ISSN 0026-1149

ISBN 0-11-728671-0



9 780117 286719

